Review

Nanoparticle-mediated synergistic anticancer effect of ferroptosis and photodynamic therapy: Novel insights and perspectives

Haiying Wang, Chu Qiao, Qiutong Guan, Minjie Wei*, Zhenhua Li*

School of Pharmacy, China Medical University, Shenyang 110122, China

ABSTRACT

Current antitumor monotherapy has many limitations, highlighting the need for novel synergistic anticancer strategies. Ferroptosis is an iron-dependent form of nonapoptotic cell death that plays a pivotal regulatory role in tumorigenesis and treatment. Photodynamic therapy (PDT) causes irreversible chemical damage to target lesions and is widely used in antitumor therapy. However, PDT's effectiveness is usually hindered by several obstacles, such as hypoxia, excess glutathione (GSH), and tumor resistance. Ferroptosis improves the anticancer efficacy of PDT by increasing oxygen and reactive oxygen species (ROS) or reducing GSH levels, and PDT also enhances ferroptosis induction due to the ROS effect in the tumor microenvironment (TME). Strategies based on nanoparticles (NPs) can subtly exploit the potential synergy of ferroptosis and PDT. This review explores recent advances and current challenges in the landscape of the underlying mechanisms regulating ferroptosis and PDT, as well as nano delivery system-mediated synergistic anticancer activity. These include polymers, biomimetic materials, metal organic frameworks (MOFs), inorganics, and carrier-free NPs. Finally, we highlight future perspectives of this novel emerging paradigm in targeted cancer therapies.

1. Introduction

Cancers significantly threaten human health because of their high morbidity and mortality. In 2023, there will be 1958,310 new cancer cases and 609,820 new cancer-related deaths in the USA [1]. Adverse effects caused by conventional treatments such as surgery, chemotherapy, and radiotherapy still critically impact on patients' quality of life [2]. Ferroptosis is an iron-dependent cell death mode characterized by a massive accumulation of lethal lipid ROS [3]. This process is significantly influenced by the presence of ferrous ions (Fe^{2+}) that mediate the Fenton reaction [4]. The Fenton reaction transforms excessive hydrogen peroxide (H_2O_2) into hydroxyl radicals ($\cdot OH$) and oxygen in the TME [5]. The resulting $\cdot OH$ triggers a cascade of free radical chain reactions,

ultimately leading to enhanced intracellular ROS levels, which cause oxidative damage to phospholipids (PLs) in the cell membrane and contribute to ferroptosis in cancer cells [6]. Additionally, ferroptosis leads to the production of highly toxic phospholipid hydroperoxides (PLOOH) through the depletion of intracellular GSH and inhibition of glutathione peroxide 4 (GPX4) [7].

Recent evidence has shown that PDT has become a promising and effective cancer therapeutic modality owing to its noninvasiveness, high spatial and temporal accuracy, strong controllability, low toxicity, and minimal immunostimulation [8]. Upon light irradiation, a photosensitizer (PS) delivers energy and electrons to react with functional intracellular biomacromolecules, generating ROS that can destroy cancer cells [9]. Furthermore, PDT enhances anticancer immunity by increasing intratumoral secretion of various proinflammatory factors and promoting T lymphocyte infiltration, leading to long-term suppression of cancer cell proliferation [10]. Hence, PDT surpasses conventional therapies, including surgery, chemotherapy, and radiotherapy [11].

However, both ferroptosis and PDT have their limitations. The high consumption of oxygen during PDT worsens hypoxia in the TME [12]. Cancer cells also express a high level of the antioxidant GSH, which inhibits ROS synthesis and significantly impacts the efficacy of PDT [13]. Ferroptosis facilitates the efficacy of PDT via producing ROS by Fenton or Fenton-like reactions that continuously generate oxygen [14]. For ferroptosis, the H_2O_2 required for the Fenton reaction is generally insufficient in tumor cells, while the ROS amount is insufficient to kill the tumor cells. In addition, tumors can exhibit intrinsic or acquired resistance to ferroptosis, restoring their vulnerability can be achieved by targeting the underlying mechanisms of resistance. The development of the PDT oxidation process results in the increase and accumulation of H_2O_2 in cells, which can serve as a reactant in the Fenton reaction [15]. Meanwhile, PDT drives ferroptosis by triggering non-enzymatic lipid peroxidation (LPO) and the production of ROS [16], which will provide insight into the molecular mechanism of PDT's immunological effects in cancer treatment. As a result of these findings, PDT and ferroptosis have synergistic rather than additive efficiencies, and the mechanisms underlying ferroptosis and PDT are shown in Fig. 1.

An increasing number of researchers are focusing on the synergistic application of ferroptosis and PDT in cancer treatment. There have been numerous reviews on ferroptosis and PDT individually, yet few have explored on their synergistic anticancer effect. Mishchenko et al. were the first to propose this effect and introduced the combined mechanism of action in a review [17]. However, the potential benefits of utilizing nano delivery systems in combined applications have yet to be discussed in detail. With the rapid development of nanotechnology, a significant advantage of multifunctional nanomaterials is that they can deliver PSs and ferroptosis inducers to target cancer while achieving synergistic therapy to increase treatment efficacy [18–20]. Therefore, a systematic summary of the nanoparticle-mediated synergistic anticancer effect of ferroptosis and PDT

is urgently needed for future development and research. Advanced NPs provide new insights into refining and improving intracellular ROS levels and reducing GSH levels, which can increase the therapeutic effects of ferroptosis and PDT and address the cancer hypoxia problem in PDT by combining various self-supply or ferroptosis oxygen strategies. Meanwhile, intelligent hypoxia-responsive and pH-responsive NPs also reduce phototoxicity by preventing premature leakage of drugs and other PSs in the TME [21]. Herein, we introduce the antitumor mechanisms of ferroptosis and PDT and their advantages and disadvantages. We then review emerging NPs for ferroptosis and PDT synergistic cancer therapy and their combination with other therapeutic modalities. Finally, we highlight the current challenges and future perspectives in the field of ferroptosis and PDT synergistic cancer therapy.

2. The mechanisms of ferroptosis and PDT for cancer therapy

2.1. The mechanism of ferroptosis

It was proposed in 2012 that ferroptosis is a distinct form of iron-dependent cell death separate from apoptosis, autophagy, necrosis, and pyroptosis. It has rapidly emerged as a promising anticancer strategy [22–24]. The metabolism of intracellular iron, amino acids, GSH, GPX4, and the peroxidation of lipids are three critical features of ferroptosis [25].

2.1.1. Iron metabolism
Iron is a crucial component in the synthesis of iron-sulfur cluster heme, and other cofactors in all eukaryotes and most prokaryotes [26]. Intracellular iron is strictly regulated by transferrin (TRF) to maintain iron homeostasis [27]. The labile iron pool (LIP) is characterized by a slight increase in Fe^{2+} accumulation in ferroptosis [28]. Cellular iron metabolism includes several processes: (1) TRF mediates the entry of extracellular iron ions (Fe^{3+}) into cells. (2) Endosomes convert Fe^{3+} to Fe^{2+} through iron reductase six-transmembrane epithelial antigen of the prostate 3 (STEAP3). (3) Divalent metal transporter one on the endosomal membrane releases Fe^{2+} into a high LIP for physiological functions, which excess Fe^{2+} is stored in ferritin. (4) Ferroportin, located on the membranes, is responsible for transporting Fe^{2+} [29]. In the Fenton reaction, the primary process involves the production of oxygen-free radicals resulting from the reaction of H_2O_2 with Fe^{2+} [30]. When intracellular Fe^{2+} levels increase, ROS and PLOOH can be generated, leading to ferroptosis [31]. Ferroptosis can be inhibited by removing iron using the iron chelating agent, deferoxamine (DFO) or by suppressing lipid ROS with ferrostatin-1 (Fer-1) [32]. Conversely, increasing intracellular iron levels with iron-bound TRF, ferric ammonium citrate, and iron chloride hexahydrate can significantly increase ferroptosis sensitivity [33]. Therefore, regulating iron metabolism represents a promising therapeutic approach to induce ferroptosis in cancer cells.
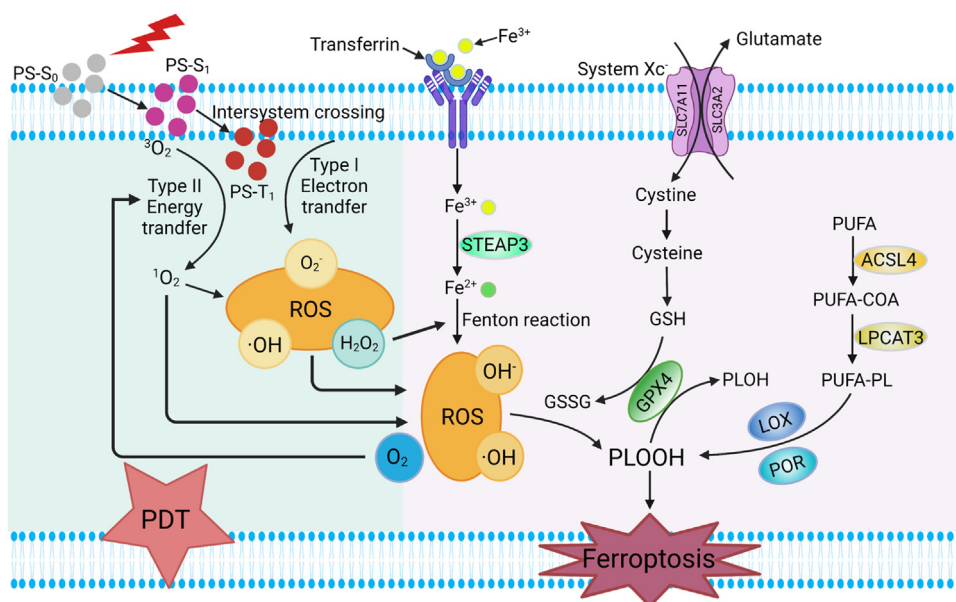
Fig. 1 – Schematic mechanism of synergistic cancer therapy of ferroptosis and PDT. Abbreviations; ACSL4: acyl-CoA synthetase long-chain family member 4; CoA: coenzyme A; Fe^{2+}: ferrous ion; Fe^{3+}: iron ion; GPX4: glutathione peroxide 4; GSH: glutathione, reduced; GSSG: glutathione, oxidized; H_2O_2: hydrogen peroxide; LOX: lipoxygenases; LPCAT3: lysophosphatidylcholine acyltransferase 3; O_2^-: superoxide anion; PDT: Photodynamic therapy; PLOH: phospholipid alcohols; PLOOH: phospholipid hydroperoxides; PL: phospholipid; POR: P450 oxidoreductase; PS: photosensitizer; PUFA: polyunsaturated fatty acid; ROS: reactive oxygen species; SLC3A2: solute carrier family 3 member 2; SLC7A11: solute carrier family 7 member 11; STEAP3: six- transmembrane epithelial antigen of the prostate 3; S_0: singlet ground state; S_1: singlet excited state; T_1: excited triplet state; $^1O_2$: singlet oxygen; •OH: hydroxyl radical.

2.1.2. Lipid metabolism

The primary feature of ferroptosis is the elevation of LPO metabolism, which can cause damage to the lipid bilayer and membrane destruction and is considered key to the ferroptosis process [34]. Polyunsaturated fatty acids (PUFAs) are a primary target of LPO, and excessive ROS lead to the accumulation of toxic PLOOH [35]. Two enzymes, acyl-coenzyme A (CoA) synthetase long-chain family member 4 (ACSL4) and lysophosphatidylcholine acyltransferase 3 (LPCAT3), play a crucial role in this process by facilitating the production, activation, and incorporation of PUFAs into membrane phospholipids (PLs) [36]. ACSL4 catalyzes the linking of long-chain PUFAs with CoA, and LPCAT3 facilitates the esterification and incorporation of these products into membrane PLs [37]. Hence, ACSL4 and LPCAT3 may be related to ferroptosis sensitivity. Enzymatic LPO involves the formation of PLOOH mediated by lipoxygenases (LOX) and cytochrome P450 oxidoreductase (POR) [38,39]. PLOOH is a product that forms when free and esterified PUFAs are deoxidized by LOX enzymes, which are non-heme iron enzyme. According to one study, cells that express 5-LOX, p12-LOX, and 15-LOX-1 are more vulnerable to ferroptosis [40].

2.1.3. Amino acid, GSH and GPX4 metabolism

The delicate balance between the cellular uptake of specific amino acids, the synthesis of GSH, and the expression level of GPX4 significantly regulate cellular ferroptosis [41,42]. Apart from ROS production by the Fenton reaction, GPX4 is also a key inhibitor of ferroptosis [43]. GPX4's role is to convert potentially lethal PLOOH into harmless phospholipid alcohols (PLOH). Therefore, direct inhibition of GPX4 activity can lead to high PLOOH levels and ultimately result in ferroptosis. Previous studies have demonstrated that GPX4 inhibitors, such as RSL3 and FIN56, directly inhibit GPX4 synthesis and ultimately result in ferroptosis [44].

GSH is a critical cofactor of GPX4, so inhibiting GSH can also cause ferroptosis [45]. The synthesis of GSH, which is critical to the activity of GPX4, requires three amino acids: cysteine, glycine, and glutamate [46,47]. As an essential component of GSH, cysteine is the rate-limiting substrate for GSH synthesis. System Xc⁻−, a transmembrane amino acid transporter with two subunits, plays a key role in introducing cysteine into cells and regulating its abundance [48]. This system consists of solute carrier family 7 member 11 (SLC7A11) and solute carrier family 3 member 2 (SLC3A2), and has potential therapeutic value for ferroptosis [49]. Erastin, the first identified ferroptosis inductor, irreversibly binds to SLC7A11 and blocks the function of system Xc⁻, ultimately leading to cysteine deficiency, GSH consumption, and endoplasmic reticulum stress [50]. Moreover, research has demonstrated that decreasing the expression of SLC7A11 results in lowered levels of GSH and cysteine, which in turn leads to an increase in ROS levels [51,52]. Cancer cells with BRCA1-associated protein 1 and p53 have been found to exhibit positive effects related to ferroptosis through the downregulation of SLC7A11 [53,54]. Other inhibitors, such as sulfasalazine and sorafenib (SRF) [55], can trigger ferroptosis by decreasing the uptake of cysteine, blocking

the synthesis of GSH, and inducing ROS accumulation [56].

2.2. The mechanism of PDT

PDT operates on the principle that specific light can excite PSs, which then transfer energy to surrounding oxygen molecules, generating $^1O_2$ and ROS, ultimately leading to irreversible and permanent death of cancer cells [57].

In cancer management, the three essential components of PDT are an appropriate light source [58], sufficient PS, and adequate oxygen [59]. An ideal PS should target cancer cells with long-term retention while being quickly eliminated from the body post-treatment [60]. PSs can be classified into three generations based on their progression [61]. The first generation of PDT PS includes hematoporphyrin derivative (HpD) or porfimer sodium (Photofrin®), which consist of porphyrin monomers, dimers, and oligomers. The second generation encompasses PS such as hypericin, chlorin e6 (Ce6), and Al (III) phthalocyanines (ZnPc). Compared to HpD, PS in the second generation shows greater selectivity for cancer cells, higher quantum yields of singlet oxygen ($^1O_2$) and tissue accumulation time, fewer adverse effects, more specific phototoxicity, and higher absorption efficiency [62]. The third generation of PS involves combining the second generation with a targeted ligand, which further increases the PDT's targeting ability, high efficiency, and safety [63]. However, an abundant supply of oxygen is a crucial requirement for PDT to be effective [64,65]. Unfortunately, the TME is typically hypoxic, which is not conducive to PDT, and further exacerbates the TME's hypoxic state [66,67].

When a photon absorption by a PS, it becomes excited and undergoes a transition from the singlet ground state (S_0) to the singlet excited state (S_1), followed by entry into the excited triplet state (T_1) [68]. The PS-intersystem involves specific mechanisms known as type I and type II [69]. Type I mechanism involves electron transfer processes that produce free radicals, resulting in increased ROS [70,71]. To produce cytotoxic $^1O_2$, the excited PS transfers its electrons to an oxygen molecule, oxidizing cells. The two mechanisms of PDT, type I and type II, differ in their oxygen dependency. Type I is an O_2-independent process [72], while type II is a highly O_2-dependent reaction [73]. The proportion of each mechanism during PDT depends on many factors, such as oxygen concentration, tissue dielectric constant, PS structure, and pH of the TME.

PDT inhibits cancer growth via three mechanisms: First, by directly damaging cancer cells. When PSs accumulate in cancer cells, the photodynamic reaction of excited PS generates ROS, leading to apoptosis, necrosis, and autophagy [74,75]. Second, by destroying surrounding blood vessels and tissues. Cancer cells have a higher proliferation rate than normal cells and require abundant nutrients from blood vessels and tissues. The photodynamic effect of PS in the TME can directly damage endothelial cell, leading to cancer cell death due to a lack of oxygen and nutrition, thereby inhibiting cancer growth [76]. Third, PDT-induced acute inflammation and the cancer immune response can lyse cancer cells, resulting in a long-term inhibitory effect on cancer growth [77].

The photodynamic induction of cancer cell death relies on various factors, including the type and concentration of PS, the location of PS targeting, the type and duration of the light source, and the oxygen level in the cancerous tissue. To improve the therapeutic efficacy of PDT, different approaches can be taken. First, PSs can be designed with specific targeting or biodegradable carriers to increase their concentration in cancer cells [78]. Determining the location and mode of PS targeting is also crucial in clarifying the mechanism of cancer cell death. Second, appropriate light source types and durations should be carefully chosen [63]. Third, increasing oxygen concentration in cancer tissues and cells is imperative [79]. To achieve this, carriers such as perfluorocarbons and hemoglobin (Hb) can be used to deliver oxygen to cancer cells [80]. Alternatively, decomposing H_2O_2 produced by cancer cells to obtain O_2 can also enhance the efficacy of PDT [81].

2.3. The relationship between the mechanisms of ferroptosis and PDT

Ferroptosis is characterized by lethal accumulation of lipid ROS, where Fe^{2+} plays an important role. The $\cdot OH$ generated by the Fenton reaction triggers free radical chain reactions, resulting in oxidative modification of cell membrane phospholipids, plasma membrane rupture, and ultimately cell death [82]. PDT has the potential to act synergistically with ferroptosis inducers, enhancing each other's effects. The ferroptosis modulators share several similarities with the cytotoxicity of ROS generated by PDT [83]. PDT-induced Type I cytotoxicity generates radical ROS and H_2O_2 through electron transfer, while type II involves the interaction of PSs with oxygen leading to the production of $^1O_2$ and H_2O_2, which further contribute to the development of oxidation processes [84]. Therefore, PDT is utilized as an H_2O_2 source to maintain the Fenton reaction, while $^1O_2$ can directly oxidize membrane lipids. In contrast, ferroptosis inducers affect the GSH-redox detoxification system [85]. The combined effect of ferroptosis and PDT generates abundant lipid ROS and leads to tumor cell death. At the same time, ferroptosis is a critical cancer cell death mechanism in PDT. Ferroptosis is primarily induced by the producing of high levels of ROS in cancer cells treated with PDT. In most cases, inducing ferroptosis in cancer cells during PDT is associated with the PS design [86]. Recent evidence has indicated that delivery systems loaded with PSs without ferroptosis inducers can indirectly and efficiently trigger ferroptosis [17].

ROS generation in PDT depends on efficient activation of PS for internalization by the targeted cells. To this end, researchers have employed Polysilsesquioxane (PSilQ) NPs loaded with PS for enhanced PDT in both *in vitro* and *in vivo* cancer treatment. These PSilQ NPs possess several noteworthy characteristics such as high PS loading, tunable surface properties, biodegradability, and biocompatibility [87]. An experiment was performed on the A375 malignant melanoma cell line to verify ROS's production, phototoxicity, and cellular internalization using nanoplatforms based on protoporphyrin IX (PpIX) called PpIX-PSilQ NPs. The study was carried out with the aim of confirming the efficacy of the PpIX-PSilQ NPs in these areas, as reported in reference [88]. Cell death induced by PDT using with PpIX-PSilQ NPs was found to occur

Table 1 – Examples of ferroptosis induced by PDT in cancer therapy.

Delivery system	PSs	Cancer cell lines	Involved ferroptosis mechanism	Refs.
Solution	IrL1	MCF-7 cells	light irradiation of the complex led to significant ferroptosis, characterized by accumulation of LPO, downregulation of GPX4, and inhibition of cell death by Fer-1. The O^{2-} and ·OH produced by IrL1 via the type I PDT process were the source of the ferroptosis pathway.	[92]
MH-PLGA-IR780 NPs	IR780	HOS cells	PDT significantly induced ferroptosis through an excessive accumulation of ROS, which caused NCOA4 activation-mediated ferritinophagy and GPX4 inactivation, synergistically resulting in excessive accumulation of lipid ROS and LPO.	[93]
Solution	RuNMe	MCF-7 cells	Cancer cells showed light-induced ferroptosis, as demonstrated by GPX4 downregulation and LPO accumulation.	[94]
Solution	TPCI	HeLa cells	TPCI activated ALOX12 to produce large amounts of lipid ROS by colocalizing with ALOX12 in multiple subcellular organelles, which triggered ferroptosis.	[95]
Solution	IrFc1	MDA-MB-231, MCF-7	After irradiation, IrFc1-induced lipid oxidation production contributes to ferroptosis in triple-negative breast cancer cells.	[96]
C-N-Ce6 NPs	Ce6	4T1 cells	Upon irradiation, Ce6 generated ROS while consuming O_2. The resulting hypoxia significantly increased the consumption of NADPH and ultimately disrupted redox homeostasis, leading to cascade amplification of ferroptosis and an increase in ROS.	[97]
Solution	TAF	Hela cells	The photoactivation of TAF resulted in cell death by triple amplifying oxidative stress through ferroptosis-apoptosis.	[98]

through a combination of ferroptosis and apoptosis. It was further established by using inhibitors, which demonstrated that ferroptosis played a significant role in the phototoxicity of NPs. These results suggested that ferroptosis was responsible for the PDT properties of PpIX-PSilQ NPs. In another study, Li et al. synthesized two near-infrared (NIR) luminophores (PI and PTI) that can generate ROS through aggregation-induced effects [89]. By manipulating the electron donor and acceptor properties of the molecules, PI model was designed as an aggregation-induced emission (AIE) active PS that emits NIR and effectively produces ROS. To enhance the intersystem crossing process via heavy atomic effects, the backbone of PI was modified with a thiophene ring to create PTI. Both PI and PTI are AIE-active PSs with excellent targeting capabilities for lipid droplets (LDs). The mechanism of cell death induced by PDT targeting LDs was elucidated by monitoring intracellular GSH and GPX4 levels. The results revealed that the oxidation of PUFAs in LDs generates LPO, leading to cellular ferroptosis.

Nitric oxide (NO) is a key signaling molecule involved in numerous bioregulation processes. Elevated levels of NO can deplete GSH, disrupting the intracellular redox balance and leading to oxidative stress, ultimately resulting in an increase in cellular ROS levels [90]. Guo et al. synthesized six derivatives of Ce6, including NO donors to enhance anticancer efficacy of PDT through the synergistic action of NO and ROS [91]. The results showed that the novel NO donors, particularly PS (PS-NO) compound, exhibited more photodynamic effects than Ce6 alone. Mechanistic studies further suggested that PS-NO can lower GSH levels, inhibiting the activity of GPX4, and promoting the accumulation of malondialdehyde when exposed to light irradiation. These finding provide evidence for a potential ferroptosis mechanism underlying the PDT effects of PS-NO. Additional examples of PDT-induced ferroptosis in the treatment of tumor are provided in Table 1.

3. Emerging nanoparticle-mediated delivery system for synergistic cancer therapy of ferroptosis and PDT

Emerging NP therapeutic strategies can effectively combine the biochemical characteristics of ferroptosis with PDT, further aggravating the damage to cellular redox balance and jointly improving the anticancer effect [99]. Polymers, biomimetic materials, MOFs, inorganics, and carrier-free NPs are used as drug delivery systems to enhance the efficacy of ferroptosis and PDT. Optimized ferroptosis and PDT could achieve a powerful synergistic effect on cancer therapy (Fig. 2).

3.1. Polymer-based NPs for synergistic therapy

Polymer-based NPs for drug delivery have attracted much attention because they significantly enhance the therapeutic effects of various kinds of medicines [100]. Poly (lactic-co-glycolic acid) (PLGA) has excellent hydrophilicity, degradability, and biocompatibility, making it a promising candidate for nanomedicine carriers [101]. Fenton reactions contribute to ferroptosis by generating large amounts of oxygen within the TME, thus alleviating hypoxia and increasing PDT effects. Researchers have found that iron-based NPs can release Fe^{2+} or Fe^{3+} in lysosomes and contribute to the intracellular Fenton reaction, producing oxygen and ROS to induce ferroptosis. Ce6, a second-generation PS in PDT, is extracted from natural chlorophyll and has the advantages of stable structure, purity, high ROS generation rate, and low phototoxicity [102]. Chen et al. developed a nanoplatform coated with Food and Drug Administration (FDA)-approved PLGA with ferrous ferric oxide (Fe_3O_4) and Ce6, which has been shown to have anticancer effects through ferroptosis and PDT (Fig. 3A) [103]. With
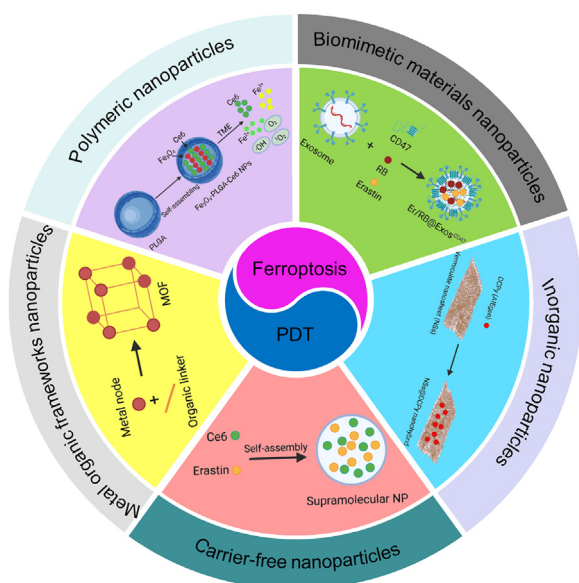
Fig. 2 – Schematic illustration of emerging NP-assisted ferroptosis and PDT for synergistic cancer therapy. The shell shows NPs, including polymeric NPs, Biomimetic NPs, MOF NPs, inorganic NPs, and carrier-free NPs.

the acidic TME, the Fe_3O_4-PLGA-Ce6 NPs can dissociate into Fe^{2+}, Fe^{3+}, and Ce6. This released Ce6 can trigger $^1O_2$ production under laser irradiation (Fig. 3B). The released Fe^{2+} and Fe^{3+} react with intracellular excess H_2O_2 in the Fenton reaction to generate ·OH (Fig. 3C), leading to intracellular ROS production (Fig. 3D) and LPO accumulation (Fig. 3E), which induce ferroptosis in cancer cells (Fig. 3F) and produce oxygen in favor of PDT. Ferroptosis often occurs in conjunction with GSH depletion, GPX4 inactivation, and an increase in ACSL4 (Fig. 3G-K) and ultimately causes highly efficient cancer cell death [104]. Following intravenous administration of Fe_3O_4 and Ce6 cargo, the combined effects of ferroptosis and PDT were highly evident due to their excellent permeability and retention capabilities. As a result, fantastic therapeutic effects with minimal adverse effects were obtained in the 4T1 breast cancer-bearing mouse model. Meanwhile, Fe_3O_4 is expected to be monitored visually by MRI of cancer therapy mediated by ferroptosis and PDT.

To take full advantage of the synergistic effects of ferroptosis and PDT, Liang et al. used a simple method to self-assemble porphyrin-grafted lipid (PGL) and DSPE-PEG in a 9:1 molar ratio onto the hydrophobic surface of oleic acid-modified Fe_3O_4 NPs (Fe_3O_4@PGL NPs) (Fig. 4A) [105]. Fe_3O_4@PGL NPs had a small size, remarkable biocompatibility, negligible dark toxicity, and high PS loading efficiency. The brilliant self-assembled properties of the as-synthesized PGL NPs promoted higher porphyrin loading. The release of iron ions directly led to the Fenton reaction, while the presence of RAW 264.7 macrophages promoted ROS production. More importantly, the influence of PDT also facilitated the Fenton reaction and oxidative stress, contributing to synergistic ROS production (Fig. 4B). The *in vitro* results indicated that low doses of Fe_3O_4@PGL NPs effectively killed tumor cells under

laser irradiation. Animal studies further illustrated that light-irradiated Fe_3O_4@PGL NPs almost wholly inhibited tumor growth by increasing ferroptosis and PDT under fluorescence and MR imaging guidance. Chen et al. designed a novel metal-free polymer PS (BDPB) to induce of ferroptosis in starved cancer cells [106]. The polymer comprises boron difluoride dipyrromethene dye as a photosensitive unit and diisopropylethylamine as an electron donor unit (Fig. 4C). Via the light-induced electron transfer process, the charge-separated polymeric photosensitizer generated complex-I mimetic activity to generate O_2^- by transferring an electron to O_2. The generated O_2^- further promoted ·OH conversion, GPX4 inactivation, and ROS accumulation, thus accelerating mitochondrial dysfunction and death of tumor cells lacking nutrients and oxygen by ferroptosis rather than necroptosis, apoptosis, or autophagy. In addition, the metal-free nature of BDBP inherently allowed for biosafety in normal cells without off-target toxicity or effected on hepatic and renal function.

In the last few years, transition metal complexes, especially Iridium (III) complexes, have been investigated extensively as promising PSs due to their excellent water solubility, brilliant photostability, strong $^1O_2$ generation, two-photon absorption, and long luminescence lifetime [107]. Ke et al. used Iridium (III) complexes to design and synthesize a biodegradable coordination polymer named IrS NPs [108]. The NPs selectively reduce GSH levels in tumor cells by decomposing into monomeric Ir^{III}, which could serve as a ROS scavenger to improve the treatment efficacy. The underlying mechanism suggested that the NPs accumulated primarily in mitochondria, where the NPs resulted in mitochondrial oxidative stress by a light-induced generation of $^1O_2$ and O_2^-, leading to mitochondrial dysfunction and fragmentation. Meanwhile, the NPs were found to generate lipid peroxides, which caused ferroptosis in tumor cells (Fig. 4D). The IrS NPs can efficiently induce synergistic cancer therapy of ferroptosis and PDT upon irradiation. Other polymer-mediated NPs for synergistic therapy are displayed in Table 2.

3.2. Biomimetic material-based NPs for synergistic therapy

Recently, biomimetic-based NPs have received increasing attention for their potential in cancer therapy. In the medical field, bionics refers to the following aspects: first, endogenous substances are extracted, separated, and purified directly from humans, animals, or microorganisms; second, synthesizing products with similar structure and function to those of the endogenous substances are synthesized; and third, a platform that mimics the disease microenvironment is constructed [111]. These strategies aim to replicate the natural pathway of the function of biological structures in organisms as much as possible. Biomimetic materials containing endogenous components or synthetic analogs of endogenous components, such as proteins, cells, and exosomes, have been generally used in tumor therapy. Compared to other nanomaterials, they exhibit many favorable properties due to their excellent biocompatibility, prominent targeting ability, low biotoxicity or immunogenicity, and degradability in tissues and cells.
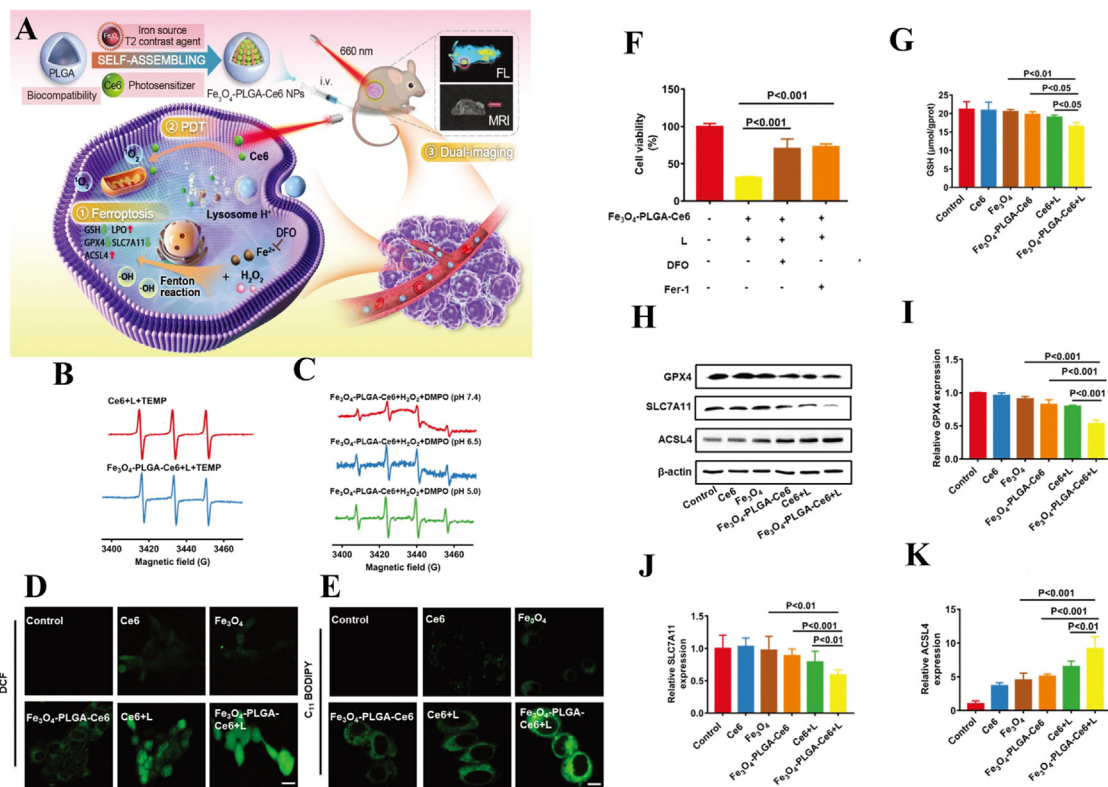
Fig. 3 – PLGA as nanocarriers in the Fenton reaction for PDT. (A) Illustration of the mechanism of Fe_3O_4-PLGA-Ce6 NPs. (B) EPR spectra resulting from the response of the two formulations. (C) The •OH produced in Fe_3O_4-PLGA-Ce6 +H_2O_2+DMPO at different pH values. (D) 4T1 breast cancer cells were treated with different drugs, irradiated for 6 h, and stained with the DCFH-DA probe by CLSM. (E) 4T1 breast cancer cells were stained with the C11 BODIPY probe for 6 h using CLSM. (F) Cell viability under laser irradiation for 24 h. (G) GSH levels when cells were treated with different preparations for 3 h. (H) Western blot analysis of GPX4, SLC7A11, and ACSL4 expression. (I-K) Gene expression of GPX4, SLC7A11, and ACSL4 by RT-qPCR after 24 h. Reprinted with permission from Ref. [103] Copyright ©2021 Royal Society of Chemistry Journal.

Table 2 – Polymer-based delivery systems for synergistic therapies of ferroptosis and PDT.

| Polymer-based Delivery System	Ferroptosis inducers	PSs	Target cancer cells	Functions	Refs.
SR780@Fe-PAE-GP	Fe^{3+}	SR780	HepG-2 cells	Ferroptosis produced ·OH and LPO, which exacerbated the oxidative stress in tumor cells and mediated cell death while depleting GSH to increase PDT.	[14]
PAF NPs	Fe^{3+}	TAPP	B16 melanoma cells	Under light irradiation, PAF showed high toxicity through intracellular ROS elevation, GSH depletion, and LPO. PAF exhibited better antitumor effects than NPs containing only Fe^{3+} or TAPP.	[15]
BNP@R	RSL-3	PPa	B16-F10 cells, 4T1 cells	NPs could implement acid-activatable PDT via protonation of the ionizable core to recruit tumor-infiltrating T lymphocytes to secrete IFN-γ, thereby sensitizing cancer cells to RSL-3-induced ferroptosis.	[109]
HA@MR@PCN–CORM	CORM-401	PCN-224	4T1 cells	Under NIR, PCN-224 was activated to generate ROS, while triggering the rapid release of intracellular CO. The CO-sensitized ferroptosis and accelerated apoptosis to effectively boost the anticancer effect of PCN-224 *in vitro* and *in vivo*.	[110]
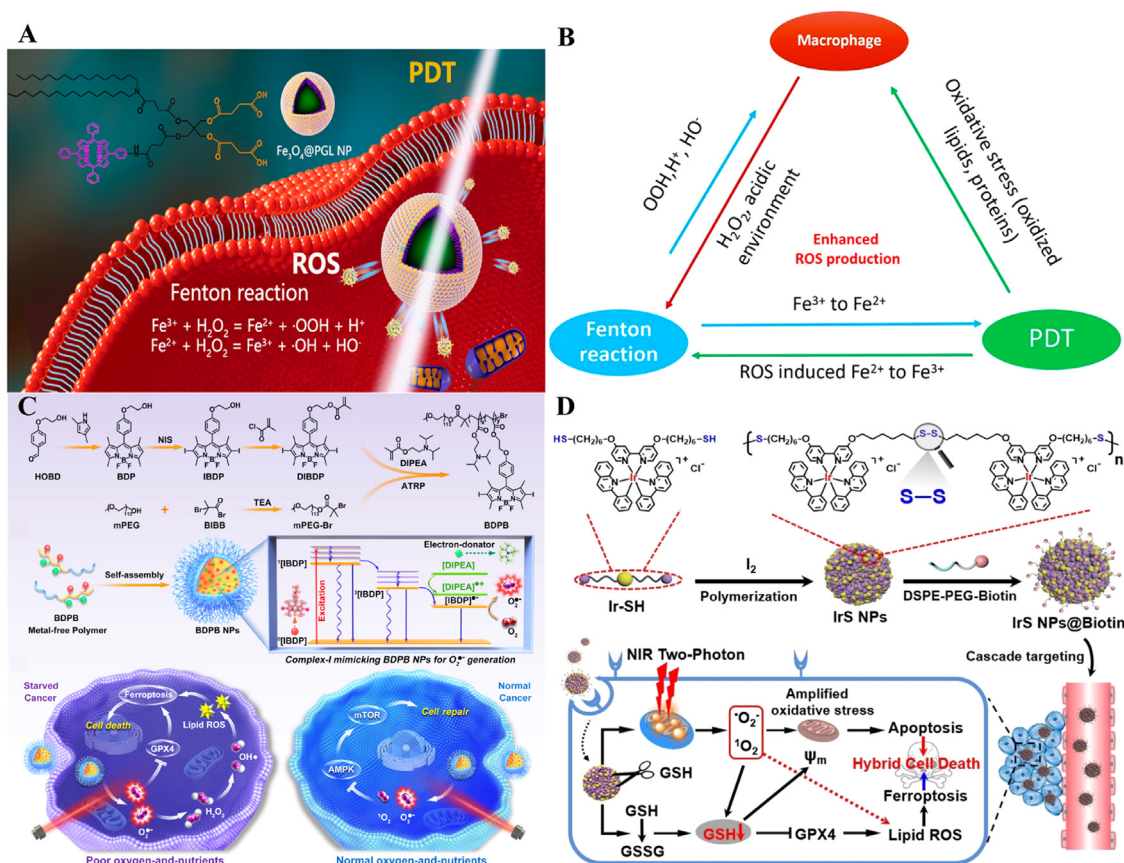
Fig. 4 – Polymers as nanocarriers for synergistic cancer therapy. (A) Schematic illustration of Fe₃O₄@PGL NPs and their mechanism. (B) Scheme of synergistic mechanism of macrophage-mediated the Fenton reaction-assisted PDT. Reprinted with permission from Ref. [105] Copyright ©2021 American Chemical Society. (C) Synthetic route of BDPB, mechanism of BDPB NPs for O₂·⁻ production and starved cancer-specific ferroptosis. Reprinted with permission from Ref. [106] Copyright ©2023 ELSEVIER. (D) Synthesis and biological mechanism of a biodegradable iridium (III) ligand polymer for two-photon PDT via a ferroptosis-apoptosis pathway. Reprinted with permission from Ref. [108] Copyright ©2022 WILEY.

3.2.1. Protein-based biomimetic NPs

Hb is a well-documented biological endogenous protein carrier used as an oxygen supplier for PDT owing to its superior ability to carry oxygen directly into hypoxic cancers [112]. Meanwhile, the iron component of Hb responsible for binding oxygen can also be applied as an iron supplement in ferroptosis therapy [113]. Hb is desirable for building a 2-in-1 NP that unifies ferroptosis and PDT. Xu et al. constructed a nanoplatform (SRF@Hb-Ce6) loaded with Hb, Ce6, and SRF (Fig. 5A) [114]. Benefiting from the innate presence of iron competent for binding oxygen, Hb simultaneously provides oxygen for O_2-dependent PDT and iron for Fe-dependent ferroptosis (Fig. 5B). SRF was recommended to self-assemble Hb-Ce6 NPs to build nanoplatforms through hydrophobic interactions and intermolecular forces. The oxygen-carrying capacity of NPs excellently improved the PDT effect and maintained the hypoxia-reversed status *in vitro* and *in vivo*. With SRF and replenishment of intrinsic iron from Hb, ferroptosis was induced because of the enhancement of PLOOH generation and significant downregulation of GPX4 [115]. As a protein-based carrier, ferritin is more prominent in cancer therapies than inorganic materials due to its inherent natural iron storage and cancer-specific recognition properties [116]. Azobenzene (AZO) groups can acquire an electron in a hypoxic environment to produce aniline derivatives, serving as hypoxia-responsive fragments [117]. Wang et al. prepared a novel hypoxia-responsive NP (BCFe@SRF) containing ferritin and SRF [118]. In the hypoxic response unit, bovine serum albumin-conjugated Ce6 (BSA-Ce6) and ferritin was covalently linked through Azo linkers to form the nanoreactor (Fig. 5C). BCFe@SRF degrades in a hypoxic environment, particularly during an oxygen-consuming PDT process. BSA-Ce6, ferritin, and SRF are released from the nanoreactor to promote PDT, catalyze the Fenton reaction, and disrupt cancer antioxidative defenses. A synergistic cancer therapy of ferroptosis and PDT using BCFe@SRF demonstrated significant therapeutic benefits both *in vitro* and *in vivo*.

3.2.2. Cell-based biomimetic NPs

Red blood cells (RBCs) are the most abundant cells in the blood and not only transport O_2 but also play an essential role in immune processes [119,120]. During RBC aging, due to the reduction of Hb and erythrocyte membrane components via vesiculation, the spleen subsequently induces the production
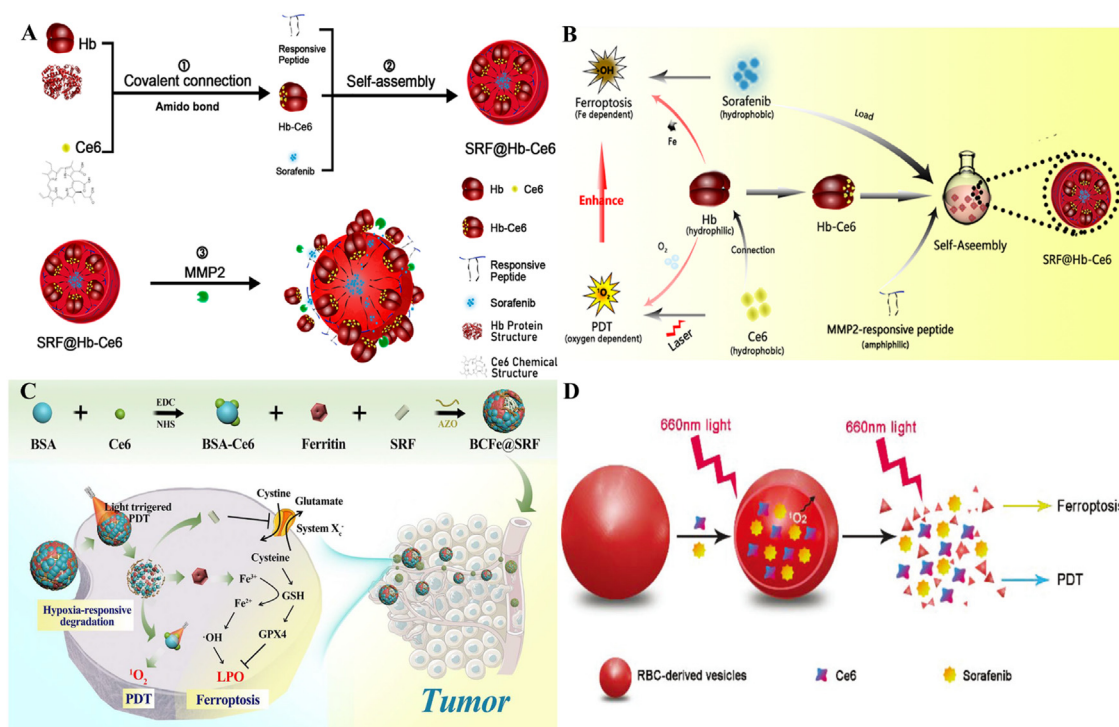
Fig. 5 – Biomimetic materials as nanocarriers for synergistic cancer therapy. (A) Construction of SRF@Hb-Ce6. (B) Oxygen-enhanced PDT and enhanced ferroptosis by SRF@Hb-Ce6. Reprinted with permission from Ref. [114] Copyright ©2020 American Chemical Society. (C) To achieve synergistic cancer therapy of ferroptosis and PDT, BCFe@SRF NPs were synthesized, and their therapeutic mechanisms were analyzed. Reprinted with permission from Ref. [118] Copyright ©2021 Creative Commons Attribution 4.0 International License. (D) The components of Ce6@SRF@RDV. Reprinted with permission from Ref. [123] Copyright ©2021 Royal Society of Chemistry Journal.

of endogenous RBC-derived vehicles (RDVs). Numerous delivery systems have been used because the Hb in RDVs can also provide oxygen and Fe^{2+} and the brilliant biocompatibility of RDVs [121]. RDVs are more lipophilic and enter the cells, but Hb has a hydrophilic shell. Apart from more helpful uptake, RDVs maximize the maintenance of Hb activity within the vesicles because they offer a natural environment that avoids the effects of chemical synthesis on Hb particles. Direct exposure to Hb is unwise because antigenicity could induce an excessive immune response and rapid clearance, whereas RDVs are milder, safer, and have sustainable effects [122]. Liu et al. designed a nanovesicle system to codeliver Ce6 and SRF into cancer cells through endocytosis of RDVs to enhance oxygen and iron, which caused stronger ferroptosis and PDT (Fig. 5D) [123]. Under local irradiation, damage to the RDV membrane resulted in the release of SRF into the cancer tissue for cancer-targeted treatment. These novel NPs boosted cancer-killing effects and safety.

3.2.3. Exosomes-based biomimetic NPs

Exosomes, tiny nanovesicles, are novel drug delivery carriers transmitting biologically active molecules between cells by proteins and nucleic acids to modulate the cellular immune system [124]. Unlike other NP carriers, exosomes include transmembrane proteins that can increase endocytosis, thus facilitating their delivery to the interior of cells [125]. As delivery vehicles, exosomes have the advantages of high biocompatibility, low immunogenicity, increased permeability and retention of cancers, and the ability to transport multiple molecules simultaneously [126]. CD47 is a ubiquitously expressed integrin-associated transmembrane protein-ligand for signal regulatory protein alpha (SIRP-α), and CD47- SIRP-α can bind to trigger the "do not eat me" signal and inhibit phagocytosis [127]. To address the phagocytosis of injected exosomes by the mononuclear phagocyte system (MPS), researchers utilized CD47 engineering to protect exosomes from phagocytosis by macrophages. Rose Bengal (RB) is a well-known PS with a high ROS yield in PDT [128]. Du et al. developed a surface-functionalized exosome nanoplatform of CD47 with high specificity to deliver erastin and RB into cancer tissues [129]. Surface functionalization of CD47 (Exos[CD47]) allowed exosomes to evade phagocytosis by MPS, thereby enhancing their accumulation in cancer tissue. Drug-loaded exosomes (Er/RB@Exos[CD47]) forcefully induced ferroptosis and PDT in cancer cells *in vitro* and *in vivo* after 532 nm laser irradiation. Therefore, engineered exosomes for synergistic therapy would be a novel strategy for treating various malignancies.

3.3. MOF-based NPs for synergistic therapy

MOFs comprising metal ions and metal clusters with organic compounds have attracted much attention due to their porous structure and prominent surface areas [130–
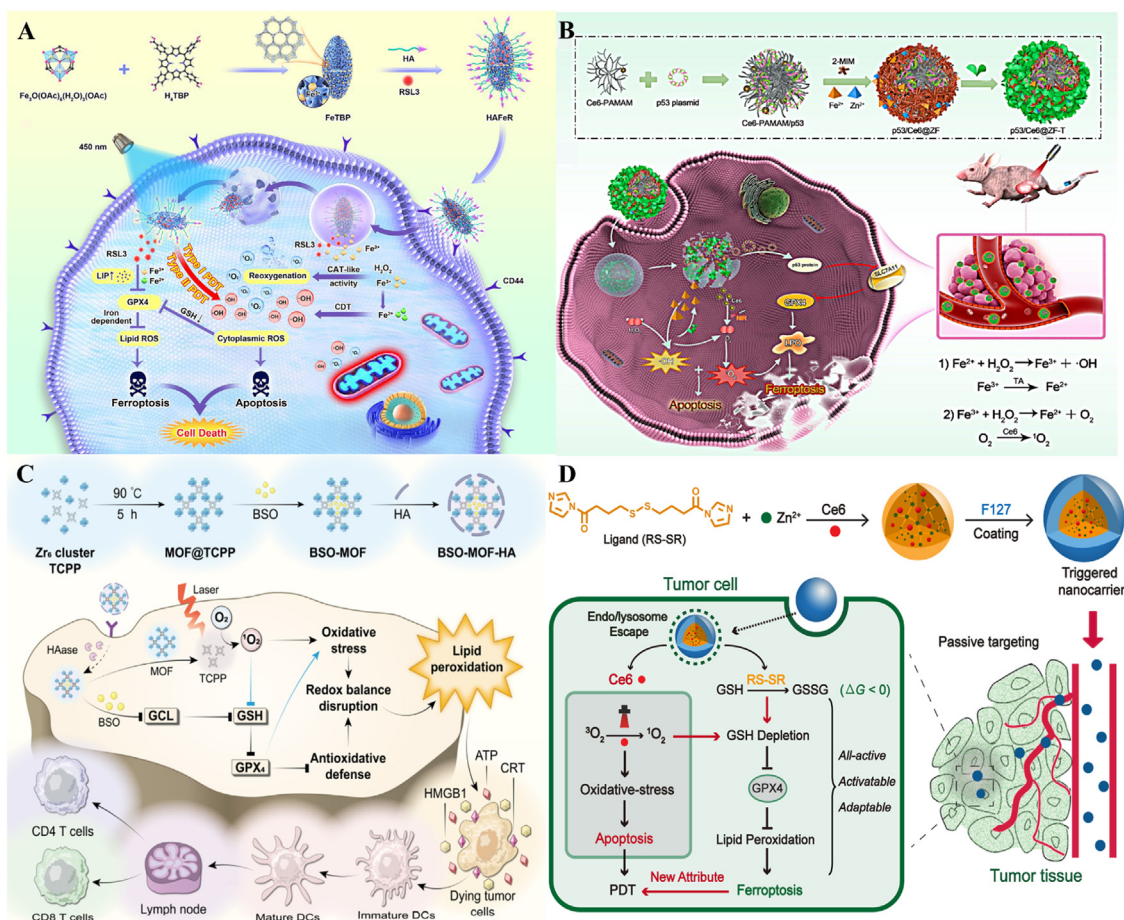
Fig. 6 – MOFs as nanocarriers for synergistic cancer therapy. (A) Synthetic route and mechanism of HAFeR NPs. Reprinted with permission from Ref. [134] Copyright ©2023 ELSEVIER. (B) Synthetic route of p53/Ce6@ZF-T and its mediation of ferroptosis and PDT. Reprinted with permission from Ref. [135] Copyright ©2022 ELSEVIER. (C) Schematic illustration of increased ferroptosis of BSO-MOF-HA. Reprinted with permission from Ref. [137] Copyright ©2023 ELSEVIER. (D) NPs with all-active MOFs for PDT involved ferroptosis and apoptosis. Reprinted with permission from Ref. [138] Copyright ©2019 American Chemical Society.

132]. Iron is a pivotal element of the Fenton reaction to generate ROS, which is positively involved in ferroptosis. Fe-MOFs have promising applications in tumor therapy, displaying better TME responses and higher dispersibility and degradability [133]. Chen et al. designed a nanocarrier, HAFeR, for synergistic ferroptosis and PDT through encapsulating RSL3 and PSs in MOFs (Fig. 6A) [134]. The HAFeR specifically recognized overexpressed CD44 on the surface of tumor cells and was internalized by receptor-mediated endocytosis. After entering acidic lysosomes, the nanocarriers were disassembled to release Fe^{2+}, Fe^{3+}, porphyrin sensitizers, and RSL3. Iron ions catalyzed H_2O_2 into O_2 through the Fenton reaction to alleviate tumor hypoxia and accelerated RSL3 to downregulate GPX4 to promote LPO, ultimately improving ROS generation for ferroptosis. HAFeR displayed high toxicity to tumor cells and effectively eradicated the tumors of MB49 tumor-bearing nude mice. Playing a vital role in the nanoplatform, MOFs achieved innovative synergistic cancer therapy of ferroptosis and PDT and exerted the best therapeutic effect. Yu et al. constructed an oxidative stress

nano delivery system named p53/Ce6@ZF-T through self-assembling Fe^{2+}, including mesoporous zeolitic imidazolate framework-8 (ZIF-8), Ce6-poly (amidoamine) (Ce6-PAMAM), and tannic acid (TA) (Fig. 6B) [135]. The NPs could be degraded when they entered cancer cells or accumulated in the TME, accompanied by the release of Fe^{2+}, Ce6, and TA. Under NIR irradiation, Fe^{2+}-mediated Fenton reaction and Ce6-mediated PDT generated large amounts of cytotoxic ROS, including ·OH and $^1O_2$. In addition, the simultaneous release of TA ensured a continuous supply of Fe^{2+} via facilitating the exchange of Fe^{3+} with Fe^{2+}, thus improving the Fenton reaction [136]. Excess intracellular ROS contributed to enhanced LPO and accelerated ferroptosis. Cationic Ce6-PAMAM complexed with p53 plasmid, accelerating ROS-mediated ferroptosis.

MOFs can also be loaded with PSs and ferroptosis inducers or substances that deplete GSH to exert the synergistic effects of ferroptosis and PDT. Wang et al. designed a Buthionine-(S, R)-sulfoximine (BSO)-loaded MOF named BSO-MOF-HA (BMH) with the combined effects of inhibiting antioxidative

defense and enhancing oxidative damage [137]. The MOF NPs were developed via the PS of [4,4,4,4-(porphine-5,10,15,20-tetrayl) tetrakis (benzoic acid)] (TCPP) and Zr6 metal ions, which were further modified with hyaluronic acid (HA) to target CD44 receptors-overexpression cancer cells (Fig. 6C). TCPP in MOF could convert light energy into chemical energy under light irradiation, enhance intracellular ROS levels and increase oxidative stress. Excessive ROS can alter intracellular redox homeostasis and enhance BSO-induced GSH depletion, GPX4 inactivation, and LPO accumulation, contributing to the synergistic effects of ferroptosis and PDT. Meng et al. designed an imidazole ligand bearing disulfide and zinc to constitute an all-active MOF nanocarrier containing Ce6 (Fig. 6D) [138]. Under light irradiation, the Ce6-encapsulated nanocarrier resulted in intracellular GSH depletion by the disulfide-thiol exchange reaction in the 4T1 mouse breast cancer cell line. Consumption of GSH also resulted in the inactivation of GPX4 and an improvement in cytotoxicity mitigated by ferroptosis inhibitors [139]. In the 4T1 breast cancer-bearing mouse model, all-active nanocarriers effectively prevented cancer growth and enhanced animal survival *in vivo*.

3.4. Inorganic-based NPs for synergistic therapy

Inorganic NPs with various tunable properties have prominent potential in nanomedicine [140]. Numerous kinds of inorganic NPs have been studied. Here, we mainly focus on silica-based NPs and other inorganic NPs for the synergistic therapy of ferroptosis and PDT.

3.4.1. Silica-based NPs

Silica-based carriers are widely used in tumor therapy due to their high specific surface area, adjustable pore morphology and size, and easy functional modification [141,142]. Silica-based NPs exhibit remarkable ion loading and responsive release capability. Currently, the commonly used silica structures are mesoporous silica NPs [143]. Tian et al. designed disulfide bond-rich mesoporous silica (MOS) NPs called HL/MOS@M780&LOD NPs, which contain linoleic acid-conjugated HA (HL), mitochondria-targeted IR780 (M780), and lactate oxidase (LOD) [144]. M780-mediated PDT and LOD-mediated starvation therapy could exacerbate effectively the hypoxic state of cancer cells, thus enhancing the levels of free iron to activate ferroptosis. Pyruvic acid and H_2O_2 produced via LOD-mediated lactate metabolism provided strong conditions for iron-catalyzed ferroptosis. Meanwhile, the depleted GSH and boosted ROS could oxidize linoleic acid into LPO to further increase ferroptosis (Fig. 7A). Li et al. constructed a mesoporous SiO_2 NP (NaYF4: Yb, Er@NaYF4@mSiO2@lipsome) based platforms via co-loading Ce6 and BSO [145]. The NPs converted NIR light to UV–vis light, which enabled the destruction of deep lesions, amplified ferroptosis, and enhanced antitumor immunity. NaYF4: Yb, Er@NaYF4@mSiO2@lipsome NPs encapsulated with Ce6 were developed to reduce the burden on the tumor sites by increasing ·OH levels and inducing apoptosis under NIR laser irradiation. Simultaneously, GSH depletion was induced via BSO co-administration and direct thiol oxidation, initiating ferroptosis. The combined strategy caused an amplification of

oxidative stress within the tumors, accompanied by intense cytotoxicity *in vitro* and *in vivo*.

3.4.2. Other inorganic-based NPs

In addition to silica-based NPs, various inorganic materials have also been used for the synergistic therapy of ferroptosis and PDT. Graphitic carbon nitride (g-C_3N_4) materials are emerging fluorescent polymeric materials composed mainly of C and N atoms [146]. Wei et al. functionalized g-C_3N_4 with Ir (III) polypyridine complexes as PS Ir-g-C_3N_4 NPs for two-photon active ferroptosis-enhanced PDT [99]. The nano-PS showed a self-sufficient and synergistic generation of oxygen from endogenous H_2O_2 and the production of $^1O_2$, ·OH, and O_2^-, which presented the capacity to solve the hypoxic TME and intervene via a multimodal mechanism by combined two-photon PDT of type I and type II. The NPs were efficiently taken up in cancer cells, where the NPs localized selectively in mitochondria. Under irradiation, Ir-g-C_3N_4 caused mitochondrial disruption and induced cell death via the combined ferroptosis and apoptosis pathways (Fig. 7B). Thus, the synergistic oxygen production method from endogenous H_2O_2 generates ROS and has excellent potential for hypoxic tumor treatment. The cell death pathway driven by ferroptosis may be valuable for treating resistant tumors and clinically challenging.

Ferrihydrite is a ubiquitous hydrated Fe (III) nano-oxide that cells use natural cellular iron storage minerals in ferritin to sustain iron homeostasis [147]. Reductive and proteolytic pathways exist for the cellular mobilization of iron from ferrihydrite in ferritin. Ferrihydrite is a heterogeneous photo-Fenton catalyst that can trigger ROS under light irradiation. Yang et al. synthesized biocompatible PEG-coated monodispersed ferrihydrite NPs (PEG-Fns) and exhibited photoactivated Fe^{2+} generation in cancer tissue (Fig. 7C) [148]. Ferrihydrite NPs with a 20-30 nm diameter have excellent biocompatibility and high cellular uptake efficiency. Under average blue light irradiation, large amounts of Fe^{2+} can be released from ferrihydrite and boost irreversible DNA fragmentation associated with iron/ROS and inhibition of GPX4, resulting in ferroptosis and apoptosis-related inhibition of cancer cell proliferation. PEG-Fns caused tumor-associated macrophage (TAM) phenotype polarization from tumor-promoting M2 to tumor-inhibiting M1 in mice. The combination of light/Fe^{2+} attenuated lung metastasis in mice by intravenous preinjection of ferrihydrite, demonstrating a new external light-controlled Fe^{2+} production method based on natural minerals. It will fully exploit the anticancer properties of Fe^{2+} in ferroptosis and PDT.

Vermiculite, a naturally layered clay, is a kind of hydrated magnesium-aluminum silicate that generally serves as a nutrient soil for bonsai [149]. AIE luminogen (AIEgen) has become fashionable as a novel PS due to its excellent luminescence performance and ROS generation [150,151]. Yu et al. developed a bonsai-vitalized oxygen-autonomous PDT system based on AIEgen/vermiculite NPs. From potted soil vermiculite, ultrathin nanosheets (NSs) were synthesized via lithium ions to produce NSs@DCPy by electrostatic suction using AIEgen PS (DCPy) (Fig. 7D) [152]. As NSs@DCPy is taken up by hypoxic cancer cells and exposed to light radiation, it can generate ·OH and $^1O_2$ and catalyze H_2O_2 to
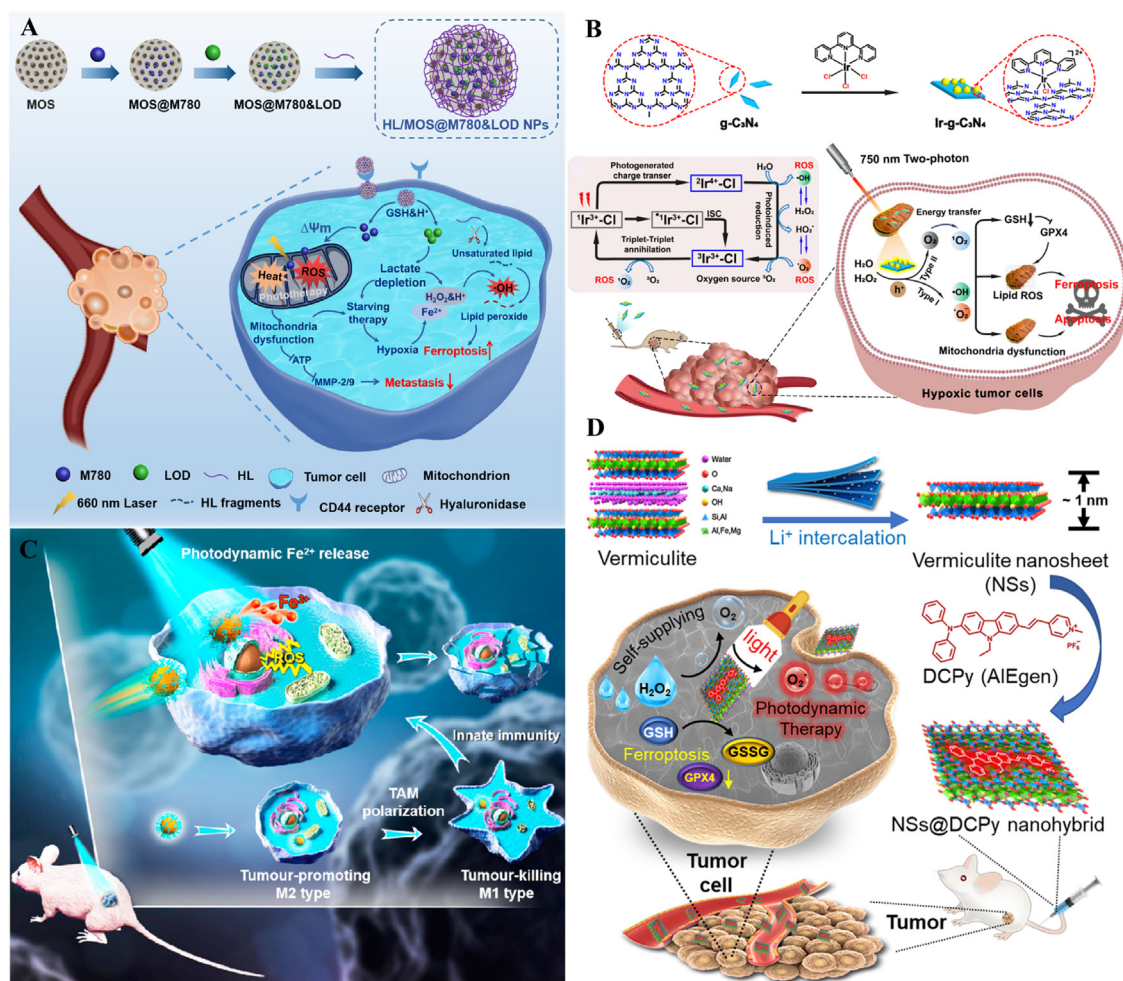
Fig. 7 – Inorganics as nanocarriers for synergistic cancer therapy. (A) Schematic illustration of the preparation and anti-metastatic properties of the HL/MOS@M780&LOD NPs. Reprinted with permission from Ref. [144] Copyright ©2022 ELSEVIER. (B) Schematic illustration of the O_2 self-sufficient nano-PS (Ir-g-C_3N_4) on production of many types of ROS ($^1O_2$, •OH, O_2^-) for ferroptosis-enhanced PDT under hypoxia. Reprinted with permission from Ref. [99] Copyright ©2022 ELSEVIER. (C) Schematic illustration of blue light-mediated Fe^{2+} release for ferroptosis and PDT. Reprinted with permission from Ref. [148] Copyright ©2022 ELSEVIER. (D) NSs@DCPy nanohybrid and its application for ferroptosis-assisted O_2 self-sufficient PDT. Reprinted with permission from Ref. [152] Copyright ©2022 ELSEVIER.

produce oxygen, enhancing the efficacy of PDT. Furthermore, NSs@DCPy induces ferroptosis by iron overload and GSH consumption and has been used in ferroptosis-assisted oxygen-independent PDT for cancer.

3.5. Carrier-free NPs for synergistic therapy

As an attractive nanodrug, carrier-free NPs are widely investigated for their simple drug compositions, high drug loading capabilities, high biosafety, and simplified synthesis procedures [153]. Zhu et al. developed a carrier-free NP (Ce6-PEG-HKN$_{15}$ NP), including Ce6 and the ferritin-homing peptide HKN$_{15}$, by a simple self-assembly method (Fig. 8A) [154]. Ce6-PEG-HKN$_{15}$ NPs accumulated around ferritin after internalization through cancer cells. Under laser irradiation, the Ce6 in NPs can effectively destroy the iron pool by

producing ROS. The released Fe^{3+} was transformed into Fe^{2+} via the high concentration of GSH (up to 10×10^{-3} M) in cancer cells. The reduced Fe^{2+} catalyzed the intracellular excess H_2O_2 derived from PDT to generate ·OH and O_2 by the Fenton reaction. The sustained production of O_2 could alleviate hypoxia in the TME and enhance PDT. Moreover, the oxidation of PUFAs led to the accumulation of LPO by highly toxic ·OH, which further disrupted redox homeostasis and induced cellular ferroptosis [155]. Zhu et al. applied Ce6 and erastin to self-assemble into a novel supramolecular carrier-free NP named Ce6-erastin by hydrogen bonding and π-π stacking (Fig. 8B) [156]. After being internalized by cancer cells, Ce6-erastin NPs demonstrated unprecedented oxygen self-sufficiency capacity to ensure effective oxygen-dependent PDT and showed excellent cytotoxicity and high ROS production. Under light irradiation, sustainable oxygen
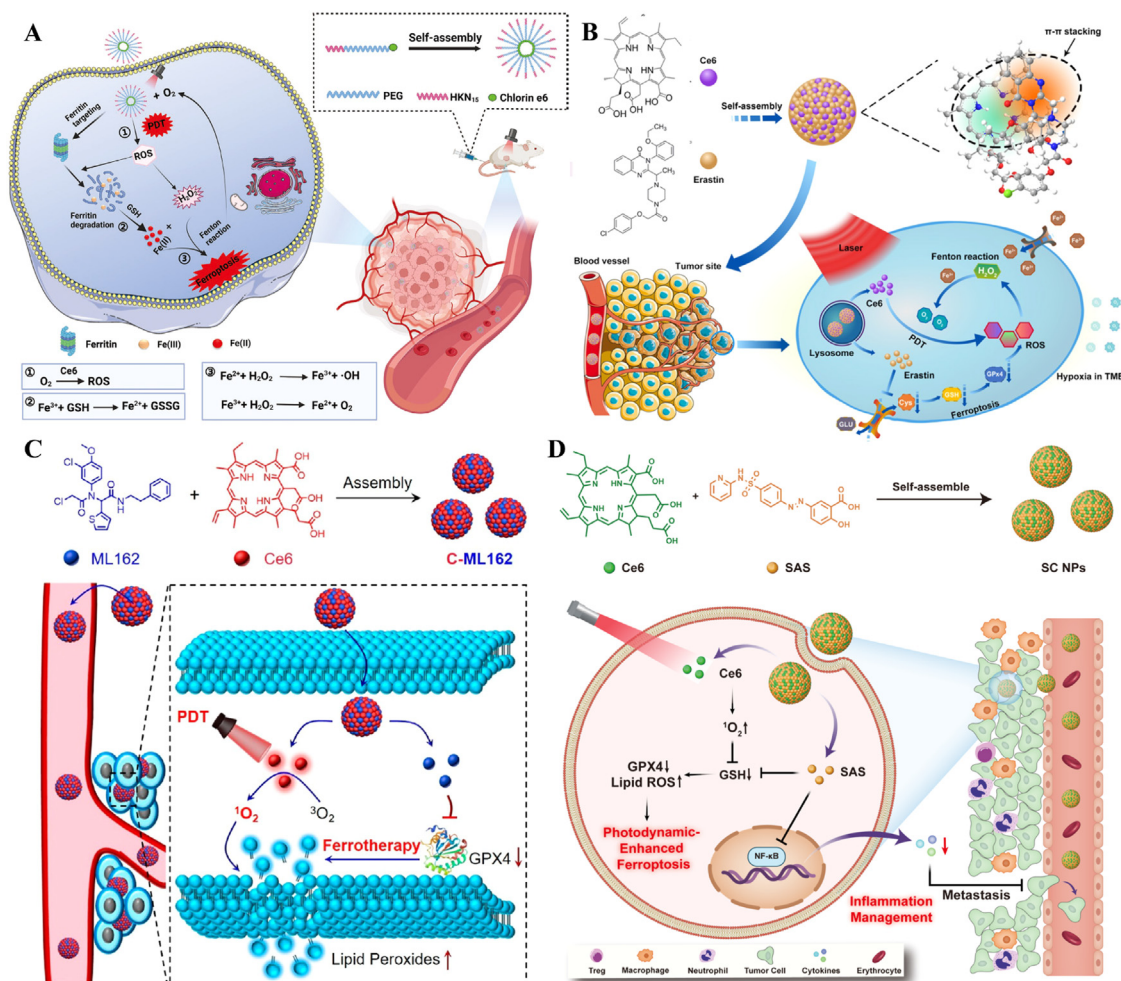
Fig. 8 – Carrier-free NPs for synergistic cancer therapy. (A) Synthetic route and mechanism of Ce6-PEG-HKN$_{15}$ NPs for ferroptosis and PDT. Reprinted with permission from Ref. [154] Copyright ©2022 WILEY. (B) Ce6-erastin NPs and their mechanism. Reprinted with permission from Ref. [156] Copyright ©2019 Creative Commons Attribution 4.0 International License. (C) The preparation process of self-assembled carrier-free C-ML162 and its synergistic therapeutic mechanism of PDT and ferroptosis. Reprinted with permission from Ref. [157] Copyright ©2022 American Chemical Society. (D) Schematic illustration of SC NPs synthesis and potential mechanism of SC NPs for tumor therapy. Reprinted with permission from Ref. [158] Copyright ©2023 ELSEVIER.

production can ensure effective photochemical reactions to trigger higher levels of ROS and cause oxidative damage to CAL-27 cells. In addition, increased PDT combined with ferroptosis can be accomplished simultaneously *in vivo*, showing remarkable anticancer capacity in CAL-27 oral squamous cell carcinoma cancer-bearing mice. Zhao et al. used a GPX4 inhibitor (ML162) and a PS (Ce6) to develop self-assembling NPs (C-ML162) via hydrophobic and electrostatic interactions to improve ferroptosis by PDT [157]. Carrier-free C-ML162 NPs enhanced antitumor drug stability, solubility, and cellular uptake. Under irradiation, internalized C-ML162 NPs produced a large amount of ROS, which oxidized intracellular unsaturated lipids to LPO. What is more, C-ML162 NPs could inactivate directly GPX4 to increase LPO accumulation, inducing ferroptosis (Fig. 8C). Meanwhile, C-ML162 NPs could accumulate at tumor sites for effective

therapy. Huang et al. reported a carrier-free NP (named SC NPs) based on the anti-inflammatory agent sulfasalazine (SAS) and Ce6 [158]. The two small molecules constituted a novel NP by supramolecular interactions, significantly enhancing the drug's biological compatibility and availability. Additionally, the SC NPs had on-demand ferroptosis induction and inflammation modulation at low dose levels compared with free drugs. Upon NP internalization in cancer cells, ferroptosis was induced by SAS-inhibited GSH generation and Ce6-mediated PDT to trigger $^1O_2$ production, which further promoted the depletion of existing GSH. The bi-directional modulation approach effectively achieved intracellular GSH depletion, which inactivated GPX4 and initiated ferroptosis (Fig. 8D). The efficient tumor therapy of these NPs came from the functional synergy of the two drugs and the delivery advantages of NPs.

4. Nanoparticle-mediated ferroptosis and PDT combined with other anticancer therapies

Although the synergistic effects of ferroptosis and PDT have demonstrated remarkable therapeutic efficacy, cancer's high heterogeneous complexity demands sophisticated therapeutic modalities [159]. To better exploit the synergistic actions of ferroptosis and PDT, more therapeutic strategies, such as chemotherapy, photothermal therapy (PTT), and chemodynamic therapy (CDT) may be combined to work against cancer cells [160,161]. Constructing a practical multiresponsive and multimodal anticancer delivery system could encapsulate different drugs into the same nanoplatform to achieve the combined application of diversified treatment methods [162].

4.1. Chemotherapy

Chemotherapy has long been the mainstay of cancer therapy. Therefore, chemotherapy and other treatments has been of great interest [163]. Researchers prepared nanomedicines of Fe-tetrakis (4-carboxyphenyl) porphyrin (Fe-TCPP) dispersed in polyvinylpyrrolidone with the hypoxia-activated drug tirapazamine (TPZ), which is coated with the cancer cell membrane (CM) as PFTT@CM [164]. PFTT@CM should escape immune clearance and accumulate preferentially in cancer tissues because it is functionalized and camouflaged by homologous cancer CM. Moreover, the acidic response properties of PFTT@CM allow it to penetrate the cells, breakdown in lysosomes, and release Fe^{3+} at the lesion site. Fe^{3+} regulated the inherent TME by catalyzing endogenous H_2O_2, reducing GSH levels, and producing $\cdot OH$ and oxygen, which could trigger ferroptosis and significantly enhance the efficacy of PDT. Furthermore, PDT stimulated by TCPP and light might deplete oxygen and exacerbate cancer hypoxia to further activate TPZ (Fig. 9A). The PFTT@CM exhibited a sequential synergistic treatment that ultimately inhibited cancer cells proliferation. Zhang et al. constructed a drug delivery system based on nanomicelles and lactose-decoration, which was loaded with triapine, a small molecule, and Ce6 to named TCLMs [165]. Ce6 and triapine displayed a combined chemo-PDT, in which both Ce6 and triapine acted synergistically as promoters of cytotoxic ROS via the Fenton reaction and NIR irradiation, respectively. Additionally, triapine could induce ferroptosis, while PDT boosted ferroptosis mediated via $^1O_2$. TCLMs exhibited increased antitumor activity in vitro and in vivo, which may be attributed to the ability of Ce6-mediated PDT and the triapine-mediated Fenton reaction to synergistically promote ROS. Mechanism studies have shown that the ROS-GSH-GPX4-LPO axis is a significant ferroptosis-inducing pathway for the antitumor effect of TCLMs.

4.2. Radiotherapy

Radiotherapy is one of the mainstream oncologic therapies alongside surgery and chemotherapy. In the current clinical protocol, approximately half of cancer patients will be treated with radiotherapy alone or in combination with other therapeutic paradigms. Radiotherapy is a critical approach in malignant tumor treatment, and its role and position are becoming increasingly prominent. The principle of radiotherapy is that high-energy ionizing radiation, including γ-rays and X-rays, interacts directly with cellular DNA, leading to DNA damage, or reacts with water molecules indirectly to generate ROS to damage DNA or others, inducing apoptosis and necrosis [166]. Liu et al. reported a simple strategy to develop mesoporous SiO_2-coated upconversion NPs (UCNPs) as nanocarriers loaded with MnO_2 and methylene blue (MB) PS for hypoxic tumor therapy [167]. The synthesized NaErF4: Yb,Gd,Eu@mSiO2/MnO2/MB@FA (Folic acid) (UPSMF/MB) has a radiosensitization effect due to the presence of high charge elements. The emission of red upconversion luminescence stimulated the coated MB to initiate PDT. In the TME, MnO_2 has catalytic activity of catalase-like, which can decompose effectively H_2O_2 into O_2, alleviating hypoxia and enhancing PDT and radiotherapy to produce ROS in the tumor area. Additionally, MnO_2 possessed remarkable glutathione peroxidase-like activity, which can breakdown effectively intracellular overexpressed GSH, thereby leading to the accumulation of LPO and inducing ferroptosis. ROS production in situ through PDT and radiotherapy further accelerated the intracellular LPO accumulation. In vitro and in vivo results showed that UPSMF/MB could inhibit significantly tumor growth via relieving tumor hypoxia and boosting PDT. Meanwhile, X-ray irradiation significantly inhibited tumor growth through alleviating tumor hypoxia and improving the radiotherapy effect. UPSMF/MB achieved 83.4% tumor suppression under the triple actions of radiotherapy, ferroptosis, and PDT with negligible toxic effects on normal cells. This study demonstrates the promising strategy of PDT associated with radiotherapy to increase ferroptosis-based synergistic therapy.

4.3. Photothermal therapy

PTT utilizes photothermal therapeutic agents (PTAs) and NIR light to kill cancer cells [168]. Light energy is absorbed by PTA and converted into heat energy, raising the lesion site's temperature to trigger cancer cell death. Cancer cells have difficulty maintaining homeostasis and die at temperatures above 45 °C [169]. Cheng et al. successfully prepared a cancer treatment nanoplatform (Fe^{3+}@Au1Ag24@PbP) with a coordinated response to NIR laser/TME [170]. The NPs consisted of precisely structured oil-soluble Au1Ag24 NCs and Fe^{3+}, easily assembled in the oil and aqueous phases of PEG block-grafted PK copolymer (PK-b-PEG, PbP) vesicles. The Au1Ag24 NCs had multiphotoresponsive properties, endowing the NPs with synergistic photodynamic and photothermal treatment capabilities and photothermal imaging abilities under NIR laser irradiation. The loaded Fe^{3+} had multi-TME reactive properties, which depleted GSH in cancer cells and catalyzed endogenous H_2O_2 decomposition in solid tumors to generate oxygen, thereby enhancing the hypoxic tumor environment and improving the PDT efficiency. Meanwhile, the produced large amount of Fe^{2+} further interacted with H_2O_2 to generate $\cdot OH$, thus realizing and enhancing the ferroptosis effect for cancer (Fig. 9B). The results confirmed that the nanoplatform guided the
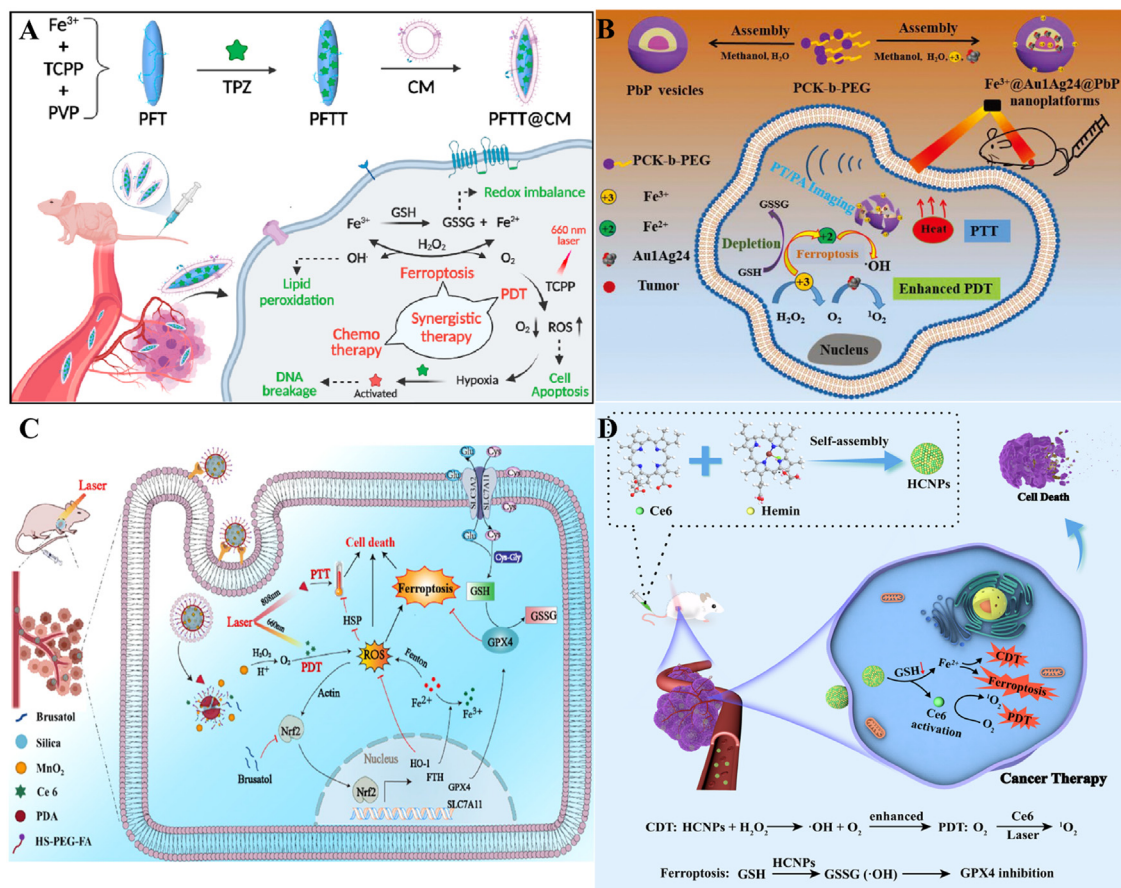
Fig. 9 – Nanoparticle-mediated ferroptosis and PDT combined with other anticancer therapies. (A) Schematic illustration of the construction of PFTT@CM and the synergistic antitumor effects of PFTT@CM combining ferroptosis, hypoxia-induced chemotherapy, and PDT. Reprinted with permission from Ref. [164] Copyright ©2022 ELSEVIER. (B) The Fe^{3+}@Au1Ag24@PbP NP formation and the imaging-guided combined antitumor treatment. Reprinted with permission from Ref. [170] Copyright ©2021 Royal Society of Chemistry Journal. (C) Schematic illustration of enhanced synergistically PDT and PTT on tumors via the combination of ferroptosis induction, ROS production, and stress-defense suppression. Reprinted with permission from Ref. [171] Copyright ©2022 American Chemical Society. (D) Schematic diagram of the preparation process of self-assembled NPs and mechanistic roles of HCNPs in combined cancer therapy. Reprinted with permission from Ref. [175] Copyright ©2021 American Chemical Society.

PDT/PTT/ferroptosis properties of trimodal cancer *in vitro* and *in vivo*. Tao et al. reported a multifunctional NP via incorporating brusatol into a silica nanonetwork. It was then modified with MnO_2 and Ce6 and followed by PEG-folate (PEG-FA) and functionalized polydopamine (PDA) (named as brusatol/silica@MnO_2/Ce6@PDA-PEG-FA) [171]. As an oxygen producer, MnO_2 can facilitate ROS generation, which increases directly Ce6-mediated PDT and enhances PDA-mediated PTT through attacking heat shock proteins [172]. Meanwhile, brusatol can inhibit effectively the activation of the Nrf2 defense pathway under hyperthermia and hyperoxidation, leading to the inactivation of GPX4 and ferritin heavy chain, thus inducing ferroptosis and increasing PDT/PTT effects ultimately (Fig. 9C). Brusatol/silica@MnO_2/Ce6@PDA-PEG-FA NPs demonstrated remarkable antitumor efficacy with improved PDT/PTT/ferroptosis *in vitro* and *in vivo*.

4.4. Chemodynamic therapy

CDT is another vital treatment method resulting in redox homeostasis dysregulation in cancer cells [173]. By explicitly binding Fenton-like reactions and the TME, CDT uses agents to convert internal H_2O_2 into toxic ·OH to kill cancer cells, demonstrating excellent therapeutic performance and a good safety profile [174]. Chen et al. developed a multifunctional NP (HCNP) that is self-assembled from two porphyrin molecules, Ce6 and hemin, driven by coordination and noncovalent effects [175]. After entering tumor cells, HCNPs generated toxic tumor $^1O_2$ under 660 nm laser irradiation for PDT. At the same time, the heme in HCNPs can catalyze the conversion of intracellular H_2O_2 to O_2 and overcome the decreased PDT effect prompted via the tumor hypoxia microenvironment, which achieved self-reinforced PDT. HCNPs can effectively deplete GSH in cancer cells and release Fe^{3+}, further

converting Fe^{3+} to Fe^{2+} through GSH-mediated redox reactions. The resulting Fe^{2+} can catalyze H_2O_2 to $\cdot OH$ by the Fenton reaction, leading to effective CDT. In addition, GSH depletion further inactivated GPX4 and induced ferroptosis (Fig. 9D). Both *in vitro* and *in vivo* results demonstrated that the combination of ferroptosis/PDT/CDT significantly achieved the highest anticancer effect under laser irradiation.

4.5. *Immunotherapy*

With advances in immunology and tumor biology, immunotherapy offers new therapeutic options for various cancers that specifically destroy tumor cells by regulating specific immune cell functions, boosting patient survival rates, and reducing adverse effects, eradicating established tumor and preventing tumor recurrence [176]. However, only a few cancer patients benefit from current immunotherapy strategies. Tumor cells often exhibit low immunogenicity to evade recognition via immune cells. Eliciting the antitumor immune response remains a challenge for cancer immunotherapy. To solve these problems, Song et al. proposed that combining PDT and GPX4 blockade can stimulate ferroptosis and promote immunotherapy subsequently, which achieved the combined effect of ferroptosis, PDT, and immunotherapy. They developed acidity-activatable dynamic NPs for fluorescence-imaging-guided PDT and tumor-targeted delivery of RSL-3 [109]. After intracellular uptake, the NPs dissociated significantly at endocytic vesicles to release RSL-3. Meanwhile, the NPs conjugated with pheophorbide (a kind of PS) had acid-activatable fluorescence and photoactivity, which enabled PDT to initiate immunogenic cell death (ICD) of cancer cells, triggering the secretion of IFN-γ, thereby accelerating GPX4-related ferroptosis via depleting system Xc$^-$ [177]. The resulting ferroptosis could initiate phagocytosis by lipid peroxide and calreticulin presentation on the tumor cell membrane surface.

4.6. *Pyroptosis*

Pyroptosis is a recently discovered mechanism of programmed cell death, characterized through continuous cell swelling until the cell rupture, which releases cellular contents. Pyroptosis is mediated via the gasdermin family of effector proteins facilitating pore formation, including gasdermin-A3 (GSDMA3), gasdermin-C (GSDMC), gasdermin-D (GSDMD), and gasdermin-E (GSDME), It is involved widely in the occurrence and development of inflammatory and infectious diseases and plays a significant role in tumor treatment. [178]. ROS production has been suggested as a classic mechanism to induce pyroptosis. Thus, pyroptosis, ferroptosis, and PDT can be combined in tumor therapy [179]. Xu et al. developed PVP-NiS$_2$/FeS$_2$ NPs, which can show synergistic effects of PDT, CDT, and PTT after NIR irradiation [180]. In addition, the photoactivity of PVP-NiS$_2$/FeS$_2$ NPs was obvious via generating abundant $^1O_2$ upon irradiation. High levels of ROS and multivalent ions promoted both pyroptosis and ferroptosis through activating GSDME and decreasing GPX4 levels, respectively. The PVP-NiS$_2$/FeS$_2$ NPs exhibit

a brilliant ferroptosis/pyroptosis/PDT/CDT/PTT synergistic therapy.

5.   Conclusions and future perspectives

Recurrence and metastasis of tumors are critical challenges. In order to overcome these challenges, many strategies have been employed to induce tumor cell apoptosis. PDT or ferroptosis has made tremendous progress in inhibiting recurrence and metastasis over the past few years [181,182]. However, there are still many obstacles before moving forward with clinical translation. Recent findings have shown that ferroptosis increases the efficacy of PDT by overcoming significant challenges, such as increasing the amount of oxygen and ROS in the TME and decreasing the level of GSH [14]. The facilitated PDT improves the potential to induce ferroptosis by boosting ROS levels. Moreover, ferroptosis induction in the PDT process has the potential to be a robust alternative strategy for improving the efficacy of cancer therapy. Integrating these unique advantages of the synergy of ferroptosis and PDT, the limitations of other cell death modalities are improved to provide more effective combined anticancer therapy.

Currently, there are very limited review articles revealing the nanoparticle-mediated synergistic anticancer effect of ferroptosis and PDT. Therefore, the current comprehensive review proposes a state-of-the-art analysis and perspectives on the synergistic effect of ferroptosis and PDT on cancer treatment efficacy. We discuss several kinds of advanced multifunctional NPs that intelligently combine ferroptosis and PDT to understand the inherent superiorities of combinational treatment that demonstrate promising therapeutic potential compared to the separate application of ferroptosis and PDT. Traditional NP-based cancer therapies, including chemotherapy and radiotherapy, can also be combined with ferroptosis and PDT to achieve ideal synergistic effects in cancer therapy. However, the following challenges and issues remain to be resolved, although NPs have made progress in the synergistic therapy of ferroptosis and PDT.

First, in addition to the mechanisms summarized in this review, a deeper understanding of synergistic therapeutic mechanisms underlying the synergistic effect of ferroptosis and PDT will provide key insights into how these combinational treatments can significantly induce the body's immune response. It was reported that fluorescence-imaging-guided PDT can trigger antitumor immune responses through enhancing the infiltration of T lymphocytes and the secretion of proinflammatory cytokines such as IFN-γ that induce ferroptosis in tumor cells, resulting in the production of antitumor immune response [183,184]. Moreover, IFN-γ inhibits the expression of SLC3A2 and SLC7A11, two subunits of the cysteine/glutamate anti-transport system Xc$^-$. This inhibition hinders intracellular GSH, triggering LPO in tumor cells. The resulting lipid peroxides serve as a "find me" signal, promoting phagocytosis of cancer cells via dendritic cells (DCs) [97]. Hence, it is essential to further explore the systemic cancer immunotherapy induced by the combination

of ferroptosis and PDT. On the other hand, ferroptosis and PDT work as "double-edged swords" for cancer treatment. For instance, ROS generated during the treatments of ferroptosis and PDT have multiple functions, including DNA damage, drug resistance, cell death, and genetic resistance, and play a pivotal role in the synergistic effect. However, they also promote cell proliferation and survival in some cases [185]. Therefore, there is an urgent need to explore the synergistic mechanisms of ferroptosis and PDT.

Second, excessive intracellular GSH has been implicated in the resistance of cancer cells to ferroptosis and PDT. When GSH is highly expressed, it can scavenge toxic ROS, thereby compromising the synergistic effect of ferroptosis and PDT. Therefore, it is preferable to compromising GSH to avoid the loss of useful ROS and enhance therapeutic efficacy. Certain chemical structures, such as disulfide bonds, trisulfide bonds, thioether bonds, selenium bonds and so on, can deplete excessive GSH and destroy the structure of NPs to release drugs. In addition, some nanocarriers such as manganese dioxide-based nanocarriers, polyoxometalate-based nanocarriers, and MOF NPs containing copper and iron, can consume GSH. Furthermore, GSH biosynthesis could be reduced by inhibition of glutamate-cysteine ligase [141]. Therefore, it is necessary to further design nano delivery systems with different GSH depletion strategies to increase the synergistic therapy of ferroptosis and PDT.

Third, tumor hypoxia is a major limiting factor for the application of PDT. Therefore, it is crucial to design nano delivery systems that can replenish, respond to, or converse oxygen. The Fenton reaction in ferroptosis can replenish oxygen by decomposing endogenous H_2O_2, but the limited catalytic efficiency of metal ions and low H_2O_2 concentrations in tumors remain unresolved challenges. To enhance the catalytic efficiency of metal ions, the local tumor temperature can be increased in combination with PTT, and H_2O_2 concentrations can be boosted through external supplementation. These strategies can overcome the limitations of the Fenton reaction and improve the efficacy of oxygen replenishment for PDT.

Fourth, the nanoparticle-mediated synergistic anticancer effect of ferroptosis and PDT has antitumor advantages. However, the development of nano delivery systems for this synergistic therapy is still in its initial stage and requires to be further investigation. Therefore, it is crucial to meticulously design and develop novel NPs with robust structures and functions for synergistic antitumor therapy of ferroptosis and PDT.

Fifth, the promising antitumor potential of ferroptosis has been well-documented. However, there are several limitations to existing small-molecule ferroptosis modulators, such as poor water solubility, short half-life *in vivo*, drug resistance and off-targeting, which hinder their clinical translation. Nanotechnology offers new opportunities to enable simultaneous delivery of ferroptosis modulators and PDT agents for tumor therapy, especially stimuli-responsive to TME nanoparticle-mediated delivery systems due to their unique spatiotemporal control properties, which will be a new direction in targeting ferroptosis and PDT. Nano delivery systems also pose many challenges for further clinical translation such as the biosafety

and degradability of nanomaterials in synergistic therapy. The preparation process of most multifunctional NPs is complicated, and introducing a good deal of chemicals to the body may raise safety concern. Although these NPs have shown encouraging results and demonstrated safety in cells and animal models such as mice or rats, this is insufficient to determine their safety in humans, which hinders clinical translation. Therefore, it is critical to conduct comprehensive toxicity studies on NPs using primates and larger animals to evaluate their safety critically for clinical translation [143]. Additionally, developing endogenous substances as delivery carriers or carrier-free NPs are also feasible strategies to improve the safety of nanocarriers.

Taken together, although significant achievements have been made in terms of the nanoparticle-mediated synergistic anticancer effect of ferroptosis and PDT, there is still more effort before they can be used in clinical practice. With the advancement of interdisciplinary research, reasonable nano delivery systems are designed to meet the needs of tumor treatment through leveraging the diverse fields of cross-collaboration, such as pharmaceutical sciences, materials science, cancer biology, immuno-oncology, biomedical engineering, and translational medicine. This review will inspire future investigations aimed at understanding additional regulatory mechanisms involved in nanoparticle-mediated combination of ferroptosis and PDT synergism, an emerging paradigm for effective cancer therapies.

Conflicts of interest

The authors report no conflicts of interest. The authors alone are responsible for the content and writing of this article.

Acknowledgements

REFERENCES

[1] Siegel RL, Miller KD, Wagle NS, Jemal A. Cancer statistics, 2023. CA Cancer J Clin 2023;73(1):17–48.

[2] Wen K, Tan H, Peng Q, Chen H, Ma H, Wang L, et al. Achieving efficient NIR-II type-I photosensitizers for photodynamic/photothermal therapy upon regulating chalcogen elements. Adv Mater 2022;34(7):e2108146.

[3] Jiang X, Stockwell BR, Conrad M. Ferroptosis: mechanisms, biology and role in disease. Nat Rev Mol Cell Biol 2021;22(4):266–82.

[4] Koo S, Park OK, Kim J, Han SI, Yoo TY, Lee N, et al. Enhanced chemodynamic therapy by Cu-Fe peroxide nanoparticles: tumor microenvironment-mediated synergistic Fenton reaction. ACS Nano 2022;16(2):2535–45.

[5] Yang Y, Zuo S, Li L, Kuang X, Li J, Sun B, et al. Iron-doxorubicin prodrug loaded liposome nanogenerator programs multimodal ferroptosis for efficient cancer therapy. Asian J Pharm Sci 2021;16(6):784–93.

[6] Meng X, Li D, Chen L, He H, Wang Q, Hong C, et al. High-performance self-cascade pyrite nanozymes for apoptosis-ferroptosis synergistic tumor therapy. ACS Nano 2021;15(3):5735–51.

[7] Yao Y, Chen Z, Zhang H, Chen C, Zeng M, Yunis J, et al. Selenium-GPX4 axis protects follicular helper T cells from ferroptosis. Nat Immunol 2021;22(9):1127–39.

[8] Li C, Zheng X, Chen W, Ji S, Yuan Y, Jiang X. Tumor microenvironment-regulated and reported nanoparticles for overcoming the self-confinement of multiple photodynamic therapy. Nano Lett 2020;20(9):6526–34.

[9] Dai J, Li Y, Long Z, Jiang R, Zhuang Z, Wang Z, et al. Efficient near-infrared photosensitizer with aggregation-induced emission for imaging-guided photodynamic therapy in multiple xenograft tumor models. ACS Nano 2020;14(1):854–66.

[10] Alzeibak R, Mishchenko TA, Shilyagina NY, Balalaeva IV, Vedunova MV, Krysko DV. Targeting immunogenic cancer cell death by photodynamic therapy: past, present and future. J Immunother Cancer 2021;9(1):e001926.

[11] Wang M, Li F, Lu T, Wu R, Yang S, Chen W. Photodynamic and ferroptotic Ce6@ZIF-8@ssPDA for head and neck cancer treatment. Mater Des 2022;224:111403.

[12] Han L, Wang Y, Huang X, Liu F, Ma C, Feng F, et al. Specific-oxygen-supply functionalized core-shell nanoparticles for smart mutual-promotion between photodynamic therapy and gambogic acid-induced chemotherapy. Biomaterials 2020;257:120228.

[13] Yoo J, Jang S-y, Park C, Lee D, Kwon S, Koo H. Lowering glutathione level by buthionine sulfoximine enhances *in vivo* photodynamic therapy using chlorin e6-loaded nanoparticles. Dyes Pigm 2020;176:108207.

[14] Sun R, Ma W, Ling M, Tang C, Zhong M, Dai J, et al. pH-activated nanoplatform for visualized photodynamic and ferroptosis synergistic therapy of tumors. J Control Release 2022;350:525–37.

[15] Li J, Li J, Pu Y, Li S, Gao W, He B. PDT-enhanced ferroptosis by a polymer nanoparticle with pH-activated singlet oxygen generation and superb biocompatibility for cancer therapy. Biomacromolecules 2021;22(3):1167–76.

[16] Shui S, Zhao Z, Wang H, Conrad M, Liu G. Non-enzymatic lipid peroxidation initiated by photodynamic therapy drives a distinct ferroptosis-like cell death pathway. Redox Biol 2021;45:102056.

[17] Mishchenko TA, Balalaeva IV, Vedunova MV, Krysko DV. Ferroptosis and photodynamic therapy synergism: enhancing anticancer treatment. Trends Cancer 2021;7(6):484–7.

[18] Peng MY, Zheng DW, Wang SB, Cheng SX, Zhang XZ. Multifunctional nanosystem for synergistic tumor therapy delivered by two-dimensional MoS2. ACS Appl Mater Interfaces 2017;9(16):13965–75.

[19] Chuang CC, Chen YN, Wang YY, Huang YC, Lin SY, Huang RY, et al. Stem cell-based delivery of gold/Chlorin e6 nanocomplexes for combined photothermal and photodynamic therapy. ACS Appl Mater Interfaces 2020;12(27):30021–30.

[20] Chen K, Li H, Zhou A, Zhou X, Xu Y, Ge H, et al. Cell membrane camouflaged metal oxide-black phosphorus biomimetic nanocomplex enhances photo-chemo-dynamic ferroptosis. ACS Appl Mater Interfaces 2022;14:26557–70.

[21] Shen L, Huang Y, Chen D, Qiu F, Ma C, Jin X, et al. pH-responsive aerobic nanoparticles for effective photodynamic therapy. Theranostics 2017;7(18):4537–50.

[22] Dixon SJ, Lemberg KM, Lamprecht MR, Skouta R, Zaitsev EM, Gleason CE, et al. Ferroptosis: an iron-dependent form of nonapoptotic cell death. Cell 2012;149(5):1060–72.

[23] Liang Y, Zhang L, Peng C, Zhang S, Chen S, Qian X, et al. Tumor microenvironments self-activated nanoscale metal-organic frameworks for ferroptosis based cancer chemodynamic/photothermal/chemo therapy. Acta Pharm Sin B 2021;11(10):3231–43.

[24] Liu Y, Song Z, Liu Y, Ma X, Wang W, Ke Y, et al. Identification of ferroptosis as a novel mechanism for antitumor activity of natural product derivative a2 in gastric cancer. Acta Pharm Sin B 2021;11(6):1513–25.

[25] Qiao C, Wang H, Guan Q, Wei M, Li Z. Ferroptosis-based nano delivery systems targeted therapy for colorectal cancer: insights and future perspectives. Asian J Pharm Sci 2022;17(5):613–29.

[26] Terzi E, Sviderskiy V, Alvarez S, Whiten G, Possemato R. Iron-sulfur cluster deficiency can be sensed by IRP2 and regulates iron homeostasis and sensitivity to ferroptosis independent of IRP1 and FBXL5. Sci Adv 2021;7:eabg4302.

[27] Gao M, Monian P, Quadri N, Ramasamy R, Jiang X. Glutaminolysis and transferrin regulate ferroptosis. Mol Cell 2015;59(2):298–308.

[28] Lin L, Wang S, Deng H, Yang W, Rao L, Tian R, et al. Endogenous labile iron pool-mediated free radical generation for cancer chemodynamic therapy. J Am Chem Soc 2020;142(36):15320–30.

[29] Zhang C, Liu X, Jin S, Chen Y, Guo R. Ferroptosis in cancer therapy: a novel approach to reversing drug resistance. Mol Cancer 2022;21(1):47.

[30] Li Y, Yang J, Gu G, Guo X, He C, Sun J, et al. Pulmonary delivery of theranostic nanoclusters for lung cancer ferroptosis with enhanced chemodynamic/radiation synergistic therapy. Nano Lett 2022;22(3):963–72.

[31] Shen Z, Liu T, Li Y, Lau J, Yang Z, Fan W, et al. Fenton-reaction-acceleratable magnetic nanoparticles for ferroptosis therapy of orthotopic brain tumors. ACS Nano 2018;12(11):11355–65.

[32] Li A, Liang C, Xu L, Wang Y, Liu W, Zhang K, et al. Boosting 5-ALA-based photodynamic therapy by a liposomal nanomedicine through intracellular iron ion regulation. Acta Pharm Sin B 2021;11(5):1329–40.

[33] Chen YC, Oses-Prieto JA, Pope LE, Burlingame AL, Dixon SJ, Renslo AR. Reactivity-based probe of the iron(II)-dependent interactome identifies new cellular modulators of ferroptosis. J Am Chem Soc 2020;142(45):19085–93.

[34] Zhang HL, Hu BX, Li ZL, Du T, Shan JL, Ye ZP, et al. PKCbetaII phosphorylates ACSL4 to amplify lipid peroxidation to induce ferroptosis. Nat Cell Biol 2022;24(1):88–98.

[35] Dierge E, Debock E, Guilbaud C, Corbet C, Mignolet E, Mignard L, et al. Peroxidation of n-3 and n-6 polyunsaturated fatty acids in the acidic tumor environment leads to ferroptosis-mediated anticancer effects. Cell Metab 2021;33(8):1701–15 e5.

[36] Chen X, Kang R, Kroemer G, Tang D. Broadening horizons: the role of ferroptosis in cancer. Nat Rev Clin Oncol 2021;18(5):280–96.

[37] Zou Y, Henry WS, Ricq EL, Graham ET, Phadnis VV, Maretich P, et al. Plasticity of ether lipids promotes ferroptosis susceptibility and evasion. Nature 2020;585(7826):603–8.

[38] Yan B, Ai Y, Sun Q, Ma Y, Cao Y, Wang J, et al. Membrane damage during ferroptosis is caused by oxidation of phospholipids catalyzed by the oxidoreductases POR and CYB5R1. Mol Cell 2021;81(2):355–69 e10.

[39] Zou Y, Li H, Graham ET, Deik AA, Eaton JK, Wang W, et al. Cytochrome P450 oxidoreductase contributes to phospholipid peroxidation in ferroptosis. Nat Chem Biol 2020;16(3):302–9.

[40] Shah R, Shchepinov MS, Pratt DA. Resolving the role of lipoxygenases in the initiation and execution of ferroptosis. ACS Cent Sci 2018;4(3):387–96.

[41] Wang WJ, Ling YY, Zhong YM, Li ZY, Tan CP, Mao ZW. Ferroptosis-enhanced cancer immunity by a ferrocene-appended iridium(III) diphosphine complex. Angew Chem Int Ed Engl 2022;61(16):e202115247.

[42] Wu J, Minikes AM, Gao M, Bian H, Li Y, Stockwell BR, et al. Intercellular interaction dictates cancer cell ferroptosis via NF2-YAP signalling. Nature 2019;572(7769):402–6.

[43] Song X, Wang X, Liu Z, Yu Z. Role of GPX4-mediated ferroptosis in the sensitivity of triple negative breast cancer cells to gefitinib. Front Oncol 2020;10:597434.

[44] Li P, Jiang M, Li K, Li H, Zhou Y, Xiao X, et al. Glutathione peroxidase 4-regulated neutrophil ferroptosis induces systemic autoimmunity. Nat Immunol 2021;22(9):1107–17.

[45] Xiong Y, Xiao C, Li Z, Yang X. Engineering nanomedicine for glutathione depletion-augmented cancer therapy. Chem Soc Rev 2021;50(10):6013–41.

[46] Kang YP, Mockabee-Macias A, Jiang C, Falzone A, Prieto-Farigua N, Stone E, et al. Non-canonical glutamate-cysteine ligase activity protects against ferroptosis. Cell Metab 2021;33(1):174–89 e7.

[47] Zhang Y, Swanda RV, Nie L, Liu X, Wang C, Lee H, et al. mTORC1 couples cyst(e)ine availability with GPX4 protein synthesis and ferroptosis regulation. Nat Commun 2021;12(1):1589.

[48] Liu J, Liu M, Zhang H, Wei X, Wang J, Xian M, et al. Exploring cysteine regulation in cancer cell survival with a highly specific "Lock and Key'' fluorescent probe for cysteine. Chem Sci 2019;10(43):10065–71.

[49] Lee H, Zandkarimi F, Zhang Y, Meena JK, Kim J, Zhuang L, et al. Energy-stress-mediated AMPK activation inhibits ferroptosis. Nat Cell Biol 2020;22(2):225–34.

[50] Wang Z, Liu Z, Wang S, Bing X, Ji X, He D, et al. Implantation of hydrogel-liposome nanoplatform inhibits glioblastoma relapse by inducing ferroptosis. Asian J Pharm Sci 2023.

[51] Zhang W, Sun Y, Bai L, Zhi L, Yang Y, Zhao Q, et al. RBMS1 regulates lung cancer ferroptosis through translational control of SLC7A11. J Clin Invest 2021;131(22):e152067.

[52] Wang H, An P, Xie E, Wu Q, Fang X, Gao H, et al. Characterization of ferroptosis in murine models of hemochromatosis. Hepatology 2017;66(2):449–65.

[53] Kain HS, Glennon EKK, Vijayan K, Arang N, Douglass AN, Fortin CL, et al. Liver stage malaria infection is controlled by host regulators of lipid peroxidation. Cell Death Differ 2020;27(1):44–54.

[54] Jiang L, Kon N, Li T, Wang SJ, Su T, Hibshoosh H, et al. Ferroptosis as a p53-mediated activity during tumour suppression. Nature 2015;520(7545):57–62.

[55] Lai Y, Lu N, Luo S, Wang H, Zhang P. A Photoactivated sorafenib-ruthenium(II) prodrug for resistant hepatocellular carcinoma therapy through ferroptosis and purine metabolism disruption. J Med Chem 2022;65(19):13041–51.

[56] Mao C, Liu X, Zhang Y, Lei G, Yan Y, Lee H, et al. DHODH-mediated ferroptosis defence is a targetable vulnerability in cancer. Nature 2021;593(7860):586–90.

[57] Du J, Shi T, Long S, Chen P, Sun W, Fan J, et al. Enhanced photodynamic therapy for overcoming tumor hypoxia: from microenvironment regulation to photosensitizer innovation. Coord Chem Rev 2021;427:213604.

[58] Li B, Lin L. Internal light source for deep photodynamic therapy. Light Sci Appl 2022;11(1):85.

[59] Sun B, Chang R, Cao S, Yuan C, Zhao L, Yang H, et al. Acid-activatable transmorphic peptide-based nanomaterials for photodynamic therapy. Angew Chem Int Ed Engl 2020;59(46):20582–8.

[60] Wang X, Tian Y, Liao X, Tang Y, Ni Q, Sun J, et al. Enhancing selective photosensitizer accumulation and oxygen supply for high-efficacy photodynamic therapy toward glioma by 5-aminolevulinic acid loaded nanoplatform. J Colloid Interface Sci 2020;565:483–93.

[61] Broadwater D, Medeiros HCD, Lunt RR, Lunt SY. Current advances in photoactive agents for cancer imaging and therapy. Annu Rev Biomed Eng 2021;23:29–60.

[62] Zhang J, Jiang C, Figueiro Longo JP, Azevedo RB, Zhang H, Muehlmann LA. An updated overview on the development of new photosensitizers for anticancer photodynamic therapy. Acta Pharm Sin B 2018;8(2):137–46.

[63] Hu T, Wang Z, Shen W, Liang R, Yan D, Wei M. Recent advances in innovative strategies for enhanced cancer photodynamic therapy. Theranostics 2021;11(7):3278–300.

[64] Ji B, Wei M, Yang B. Recent advances in nanomedicines for photodynamic therapy (PDT)-driven cancer immunotherapy. Theranostics 2022;12(1):434–58.

[65] Huang H, Banerjee S, Qiu K, Zhang P, Blacque O, Malcomson T, et al. Targeted photoredox catalysis in cancer cells. Nat Chem 2019;11(11):1041–8.

[66] Huang X, Zhang W, Peng Y, Gao L, Wang F, Wang L, et al. A multifunctional layered nickel silicate nanogenerator of synchronous oxygen self-supply and superoxide radical generation for hypoxic tumor therapy. ACS Nano 2021;16:974–83.

[67] Gilson RC, Black KCL, Lane DD, Achilefu S. Hybrid TiO_2 -ruthenium nano-photosensitizer synergistically produces reactive oxygen species in both hypoxic and normoxic conditions. Angew Chem Int Ed Engl 2017;56(36):10717–20.

[68] Bevernaegie R, Doix B, Bastien E, Diman A, Decottignies A, Feron O, et al. Exploring the phototoxicity of hypoxic active iridium(III)-based sensitizers in 3D tumor spheroids. J Am Chem Soc 2019;141(46):18486–91.

[69] Li X, Lee D, Huang JD, Yoon J. Phthalocyanine-assembled nanodots as photosensitizers for highly efficient type I photoreactions in photodynamic therapy. Angew Chem Int Ed Engl 2018;57(31):9885–90.

[70] Meng L, Cheng Y, Tong X, Gan S, Ding Y, Zhang Y, et al. Tumor oxygenation and hypoxia inducible factor-1 functional inhibition via a reactive oxygen species responsive nanoplatform for enhancing radiation therapy and abscopal effects. ACS Nano 2018;12(8):8308–22.

[71] Lv Z, Wei H, Li Q, Su X, Liu S, Zhang KY, et al. Achieving efficient photodynamic therapy under both normoxia and hypoxia using cyclometalated Ru(ii) photosensitizer through type I photochemical process. Chem Sci 2018;9(2):502–12.

[72] An J, Tang S, Hong G, Chen W, Chen M, Song J, et al. An unexpected strategy to alleviate hypoxia limitation of photodynamic therapy by biotinylation of photosensitizers. Nat Commun 2022;13(1):2225.

[73] Huang H, Xie W, Wan Q, Mao L, Hu D, Sun H, et al. A self-degradable conjugated polymer for photodynamic therapy with reliable postoperative safety. Adv Sci (Weinh) 2022;9(4):e2104101.

[74] Sun Y, Zhao D, Wang G, Wang Y, Cao L, Sun J, et al. Recent progress of hypoxia-modulated multifunctional nanomedicines to enhance photodynamic therapy: opportunities, challenges, and future development. Acta Pharm Sin B 2020;10(8):1382–96.

[75] Bansal A, Yang F, Xi T, Zhang Y, Ho JS. *In vivo* wireless photonic photodynamic therapy. Proc Natl Acad Sci USA 2018;115(7):1469–74.

[76] Deng K, Yu H, Li JM, Li KH, Zhao HY, Ke M, et al. Dual-step irradiation strategy to sequentially destroy singlet oxygen-responsive polymeric micelles and boost photodynamic cancer therapy. Biomaterials 2021;275:120959.

[77] Sun F, Zhu Q, Li T, Saeed M, Xu Z, Zhong F, et al. Regulating glucose metabolism with prodrug nanoparticles for

promoting photoimmunotherapy of pancreatic cancer. Adv Sci 2021;8(4):2002746.

[78] Pham TC, Nguyen VN, Choi Y, Lee S, Yoon J. Recent strategies to develop innovative photosensitizers for enhanced photodynamic therapy. Chem Rev 2021;121(21):13454–619.

[79] Liu LH, Zhang YH, Qiu WX, Zhang L, Gao F, Li B, et al. Dual-stage light amplified photodynamic therapy against hypoxic tumor based on an O_2 self-sufficient nanoplatform. Small 2017;13(37):1701621.

[80] Liang X, Chen M, Bhattarai P, Hameed S, Dai Z. Perfluorocarbon@Porphyrin nanoparticles for tumor hypoxia relief to enhance photodynamic therapy against liver metastasis of colon cancer. ACS Nano 2020;14(10):13569–83.

[81] Chen H, Tian J, He W, Guo Z. H_2O_2-activatable and O_2-evolving nanoparticles for highly efficient and selective photodynamic therapy against hypoxic tumor cells. J Am Chem Soc 2015;137(4):1539–47.

[82] Yang WS, Kim KJ, Gaschler MM, Patel M, Shchepinov MS, Stockwell BR. Peroxidation of polyunsaturated fatty acids by lipoxygenases drives ferroptosis. Proc Natl Acad Sci U S A 2016;113(34):E4966–75.

[83] Yang Y, Zeng Z, Almatrafi E, Huang D, Zhang C, Xiong W, et al. Core-shell structured nanoparticles for photodynamic therapy-based cancer treatment and related imaging. Coord Chem Rev 2022;458:214427.

[84] Li X, Chen L, Huang M, Zeng S, Zheng J, Peng S, et al. Innovative strategies for photodynamic therapy against hypoxic tumor. Asian J Pharm Sci 2023;18(1):100775.

[85] Zhang Z, Ji Y, Hu N, Yu Q, Zhang X, Li J, et al. Ferroptosis-induced anticancer effect of resveratrol with a biomimetic nano-delivery system in colorectal cancer treatment. Asian J Pharm Sci 2022;17(5):751–66.

[86] Han N, Li LG, Peng XC, Ma QL, Yang ZY, Wang XY, et al. Ferroptosis triggered by dihydroartemisinin facilitates chlorin e6 induced photodynamic therapy against lung cancerthrough inhibiting GPX4 and enhancing ROS. Eur J Pharmacol 2022;919:174797.

[87] Vega DL, Lodge P, Vivero-Escoto JL. Redox-responsive porphyrin-based polysilsesquioxane nanoparticles for photodynamic therapy of cancer cells. Int J Mol Sci 2015;17(1):56.

[88] Vadarevu H, Juneja R, Lyles Z, Vivero-Escoto JL. Light-activated protoporphyrin IX-based polysilsesquioxane nanoparticles induce ferroptosis in melanoma cells. Nanomaterials 2021;11(9):2324.

[89] Li Y, Zhang R, Wan Q, Hu R, Ma Y, Wang Z, et al. Trojan horse-like nano-AIE aggregates based on homologous targeting strategy and their photodynamic therapy in anticancer application. Adv Sci 2021;8(23): e2102561.

[90] Hu D, Deng Y, Jia F, Jin Q, Ji J. Surface charge switchable supramolecular nanocarriers for nitric oxide synergistic photodynamic eradication of biofilms. ACS Nano 2020;14(1):347–59.

[91] Guo X, Yu H, Shen W, Cai R, Li Y, Li G, et al. Synthesis and biological evaluation of NO-donor containing photosensitizers to induce ferroptosis of cancer cells. Bioorg Chem 2021;116:105355.

[92] Yuan H, Han Z, Chen Y, Qi F, Fang H, Guo Z, et al. Ferroptosis photoinduced by new cyclometalated iridium(III) complexes and its synergism with apoptosis in tumor cell inhibition. Angew Chem 2021;133(15):8255–62.

[93] Wang Y, Zhang L, Zhao G, Zhang Y, Zhan F, Chen Z, et al. Homologous targeting nanoparticles for enhanced PDT against osteosarcoma HOS cells and the related molecular mechanisms. J Nanobiotechnol 2022;20(1):83.

[94] Qi F, Yuan H, Chen Y, Peng X-X, Wu Y, He W, et al. Type I photoreaction and photoinduced ferroptosis by a Ru(II) complex to overcome tumor hypoxia in photodynamic therapy. CCS Chemistry 2022:1–9.

[95] Wang X, Chen Y, Yang X, Cheng L, He Z, Xin Y, et al. Activation of ALOX12 by a multi-organelle-orienting photosensitizer drives ACSL4-independent cell ferroptosis. Cell Death Dis 2022;13(12):1040.

[96] Ling YY, Wang WJ, Hao L, Wu XW, Liang JH, Zhang H, et al. Self-amplifying iridium(III) photosensitizer for ferroptosis-mediated immunotherapy against transferrin receptor-overexpressing cancer. Small 2022;18(49):e2203659.

[97] Yu F, Shang X, Wang Z, Zhu Y, Chen S, Yuan H, et al. Drug-independent NADPH-consuming micelles collaborate with ROS-generator for cascade ferroptosis amplification by impairing redox homeostasis. Mater Today Bio 2023;18:100532.

[98] Peng J, Du K, Sun J, Yang X, Wang X, Zhang X, et al. Photocatalytic generation of hydrogen radical (H·) with GSH for photodynamic therapy. Angew Chem Int Ed Engl 2023;62(9):e202214991.

[99] Wei F, Karges J, Shen J, Xie L, Xiong K, Zhang X, et al. A mitochondria-localized oxygen self-sufficient two-photon nano-photosensitizer for ferroptosis-boosted photodynamic therapy under hypoxia. Nano Today 2022;44:101509.

[100] George A, Shah PA, Shrivastav PS. Natural biodegradable polymers based nano-formulations for drug delivery: a review. Int J Pharm 2019;561:244–64.

[101] Maadani AM, Salahinejad E. Performance comparison of PLA- and PLGA-coated porous bioceramic scaffolds: mechanical, biodegradability, bioactivity, delivery and biocompatibility assessments. J Control Release 2022;351:1–7.

[102] Zheng Y, Ye J, Li Z, Chen H, Gao Y. Recent progress in sono-photodynamic cancer therapy: from developed new sensitizers to nanotechnology-based efficacy-enhancing strategies. Acta Pharm Sin B 2021;11(8):2197–219.

[103] Chen Q, Ma X, Xie L, Chen W, Xu Z, Song E, et al. Iron-based nanoparticles for MR imaging-guided ferroptosis in combination with photodynamic therapy to enhance cancer treatment. Nanoscale 2021;13(9):4855–70.

[104] Lei G, Zhang Y, Koppula P, Liu X, Zhang J, Lin SH, et al. The role of ferroptosis in ionizing radiation-induced cell death and tumor suppression. Cell Res 2020;30(2):146–62.

[105] Liang X, Chen M, Bhattarai P, Hameed S, Tang Y, Dai Z. Complementing cancer photodynamic therapy with ferroptosis through iron oxide loaded porphyrin-grafted lipid nanoparticles. ACS Nano 2021;15(12):20164–80.

[106] Chen D, Liang C, Qu X, Zhang T, Mou X, Cai Y, et al. Metal-free polymer nano-photosensitizer actuates ferroptosis in starved cancer. Biomaterials 2023;292:121944.

[107] Kuang S, Wei F, Karges J, Ke L, Xiong K, Liao X, et al. Photodecaging of a mitochondria-localized iridium(III) endoperoxide complex for two-photon photoactivated therapy under hypoxia. J Am Chem Soc 2022;144(9):4091–101.

[108] Ke L, Wei F, Xie L, Karges J, Chen Y, Ji L, et al. A biodegradable iridium(III) coordination polymer for enhanced two-photon photodynamic therapy using an apoptosis-ferroptosis hybrid pathway. Angew Chem Int Ed Engl 2022;61(28):e202205429.

[109] Song R, Li T, Ye J, Sun F, Hou B, Saeed M, et al. Acidity-activatable dynamic nanoparticles boosting ferroptotic cell death for immunotherapy of cancer. Adv Mater 2021;33(31):e2101155.

[110] Yang F, Yu W, Yu Q, Liu X, Liu C, Lu C, et al. Mitochondria-targeted nanosystem with reactive oxygen species-controlled release of CO to enhance photodynamic therapy of PCN-224 by sensitizing ferroptosis. Small 2023:e2206124.

[111] Li A, Zhao J, Fu J, Cai J, Zhang P. Recent advances of biomimetic nano-systems in the diagnosis and treatment of tumor. Asian J Pharm Sci 2021;16(2):161–74.

[112] Xiao X, Chen M, Zhang Y, Li L, Peng Y, Zhou W, et al. Hemin-incorporating DNA nanozyme enabling catalytic oxygenation and GSH depletion for enhanced photodynamic therapy and synergistic tumor ferroptosis. J Nanobiotechnol 2022;20(1):410.

[113] Liu WL, Liu T, Zou MZ, Yu WY, Li CX, He ZY, et al. Aggressive man-made red blood cells for hypoxia-resistant photodynamic therapy. Adv Mater 2018;30(35):e1802006.

[114] Xu T, Ma Y, Yuan Q, Hu H, Hu X, Qian Z, et al. Enhanced ferroptosis by oxygen-boosted phototherapy based on a 2-in-1 nanoplatform of ferrous hemoglobin for tumor synergistic therapy. ACS Nano 2020;14(3):3414–25.

[115] Liu T, Liu W, Zhang M, Yu W, Gao F, Li C, et al. Ferrous-supply-regeneration nanoengineering for cancer-cell-specific ferroptosis in combination with imaging-guided photodynamic therapy. ACS Nano 2018;12(12):12181–92.

[116] Hou W, Xie Y, Song X, Sun X, Lotze MT, Zeh HJ 3rd, et al. Autophagy promotes ferroptosis by degradation of ferritin. Autophagy 2016;12(8):1425–8.

[117] Verwilst P, Han J, Lee J, Mun S, Kang HG, Kim JS. Reconsidering azobenzene as a component of small-molecule hypoxia-mediated cancer drugs: a theranostic case study. Biomaterials 2017;115:104–14.

[118] Wang X, Wu M, Zhang X, Li F, Zeng Y, Lin X, et al. Hypoxia-responsive nanoreactors based on self-enhanced photodynamic sensitization and triggered ferroptosis for cancer synergistic therapy. J Nanobiotechnol 2021;19(1):204.

[119] Pei Q, Hu X, Zheng X, Liu S, Li Y, Jing X, et al. Light-activatable red blood cell membrane-camouflaged dimeric prodrug nanoparticles for synergistic photodynamic/chemotherapy. ACS Nano 2018;12(2):1630–41.

[120] Wu M, Ling W, Wei J, Liao R, Sun H, Li D, et al. Biomimetic photosensitizer nanocrystals trigger enhanced ferroptosis for improving cancer treatment. J Control Release 2022;352:1116–33.

[121] Han X, Shen S, Fan Q, Chen G, Edikan A, Gianpietro D, et al. Red blood cell-derived nanoerythrosome for antigen delivery with enhanced cancer immunotherapy. Sci Adv 2019;5:eaaw6870.

[122] Wu SH, Hsieh CC, Hsu SC, Yao M, Hsiao JK, Wang SW, et al. RBC-derived vesicles as a systemic delivery system of doxorubicin for lysosomal-mitochondrial axis-improved cancer therapy. J Adv Res 2021;30:185–96.

[123] Liu W, Zhang J, Ding L, Ni W, Yuan J, Xiao H, et al. RBC-derived nanosystem with enhanced ferroptosis triggered by oxygen-boosted phototherapy for synergized tumor treatment. Biomater Sci 2021;9(21):7228–36.

[124] Kalluri R, LeBleu VS. The biology, function, and biomedical applications of exosomes. Science 2020;367(6478):637–9.

[125] Kamerkar S, LeBleu VS, Sugimoto H, Yang S, Ruivo CF, Melo SA, et al. Exosomes facilitate therapeutic targeting of oncogenic KRAS in pancreatic cancer. Nature 2017;546(7659):498–503.

[126] Yang Z, Shi J, Xie J, Wang Y, Sun J, Liu T, et al. Large-scale generation of functional mRNA-encapsulating exosomes via cellular nanoporation. Nat Biomed Eng 2020;4(1):69–83.

[127] Nie W, Wu G, Zhang J, Huang LL, Ding J, Jiang A, et al. Responsive exosome nano-bioconjugates for synergistic cancer therapy. Angew Chem Int Ed Engl 2020;59(5):2018–22.

[128] Chen G, Jaskula-Sztul R, Esquibel CR, Lou I, Zheng Q, Dammalapati A, et al. Neuroendocrine tumor-targeted upconversion nanoparticle-based micelles for simultaneous NIR-controlled combination chemotherapy and photodynamic therapy, and fluorescence imaging. Adv Funct Mater 2017;27(8):1604671.

[129] Du J, Wan Z, Wang C, Lu F, Wei M, Wang D, et al. Designer exosomes for targeted and efficient ferroptosis induction in cancer via chemo-photodynamic therapy. Theranostics 2021;11(17):8185–96.

[130] Li K, Lin C, Li M, Xu K, He Y, Mao Y, et al. Multienzyme-like reactivity cooperatively impairs glutathione peroxidase 4 and ferroptosis suppressor protein 1 pathways in triple-negative breast cancer for sensitized ferroptosis therapy. ACS Nano 2022;16(2):2381–98.

[131] Liu J, Huang J, Zhang L, Lei J. Multifunctional metal-organic framework heterostructures for enhanced cancer therapy. Chem Soc Rev 2021;50(2):1188–218.

[132] Wang D, Wu H, Lim WQ, Phua SZF, Xu P, Chen Q, et al. A mesoporous nanoenzyme derived from metal-organic frameworks with endogenous oxygen generation to alleviate tumor hypoxia for significantly enhanced photodynamic therapy. Adv Mater 2019;31(27):e1901893.

[133] Zhang X, Ge H, Ma Y, Song L, Ma Y, Tian G, et al. Engineered anti-cancer nanomedicine for synergistic ferroptosis-immunotherapy. Chem Eng J 2023;455:140688.

[134] Chen Y, Gu L, Ma B, Li X, Mei Y, Zhou J, et al. Photoactivatable metal organic framework for synergistic ferroptosis and photodynamic therapy using 450nm laser. Chem Eng J 2023;454:140438.

[135] Yu M, Yu J, Yi Y, Chen T, Yu L, Zeng W, et al. Oxidative stress-amplified nanomedicine for intensified ferroptosis-apoptosis combined tumor therapy. J Control Release 2022;347:104–14.

[136] Zhou K, Xu W, Zhang X, Wang S, Li Y, Yang L, et al. Complex of nanocarriers based on the metal polyphenol network: multi-modal synergistic inhibition of tumor cell proliferation by inducing ferroptosis and photodynamic effect. New J Chem 2022;46(45):21962–7.

[137] Wang C, Wang J, Pan X, Yu S, Chen M, Gao Y, et al. Reversing ferroptosis resistance by MOFs through regulation intracellular redox homeostasis. Asian J Pharm Sci 2023;18(1):100770.

[138] Meng X, Deng J, Liu F, Guo T, Liu M, Dai P, et al. Triggered all-active metal organic framework: ferroptosis machinery contributes to the apoptotic photodynamic antitumor therapy. Nano Lett 2019;19(11):7866–76.

[139] Liang X, Mu M, Chen B, Chuan D, Zhao N, Fan R, et al. BSA-assisted synthesis of nanoreactors with dual pH and glutathione responses for ferroptosis and photodynamic synergistic therapy of colorectal cancer. Mater Today Adv 2022;16:100308.

[140] Yang G, Phua SZF, Bindra AK, Zhao Y. Degradability and clearance of inorganic nanoparticles for biomedical applications. Adv Mater 2019;31(10):e1805730.

[141] Xu Q, Yang Y, Lu J, Lin Y, Feng S, Luo X, et al. Recent trends of mesoporous silica-based nanoplatforms for nanodynamic therapies. Coord Chem Rev 2022;469:214687.

[142] Wang K, Lu J, Li J, Gao Y, Mao Y, Zhao Q, et al. Current trends in smart mesoporous silica-based nanovehicles for photoactivated cancer therapy. J Control Release 2021;339:445–72.

[143] Lu J, Yang Y, Xu Q, Lin Y, Feng S, Mao Y, et al. Recent advances in multi-configurable nanomaterials for improved chemodynamic therapy. Coord Chem Rev 2023;474:214861.

[144] Tian H, Zhou L, Wang Y, Nice EC, Huang C, Zhang H. A targeted nanomodulator capable of manipulating tumor microenvironment against metastasis. J Control Release 2022;348:590–600.

[145] Li D, Ren J, Li J, Zhang Y, Lou Y, Zhu J, et al. Ferroptosis-apoptosis combined anti-melanoma immunotherapy with a NIR-responsive upconverting mSiO2 photodynamic platform. Chem Eng J 2021;419:129557.

[146] Liao G, He F, Li Q, Zhong L, Zhao R, Che H, et al. Emerging graphitic carbon nitride-based materials for biomedical applications. Prog Mater Sci 2020;112:100666.

[147] Michel FM, Ehm L, Antao SM, Lee PL, Chupas PJ, Liu G, et al. The structure of ferrihydrite, a nanocrystalline material. Science 2007;316(5832):1726–9.

[148] Yang Y, Tian Q, Wu S, Li Y, Yang K, Yan Y, et al. Blue light-triggered Fe(2+)-release from monodispersed ferrihydrite nanoparticles for cancer iron therapy. Biomaterials 2021;271:120739.

[149] Ji X, Ge L, Liu C, Tang Z, Xiao Y, Chen W, et al. Capturing functional two-dimensional nanosheets from sandwich-structure vermiculite for cancer theranostics. Nat Commun 2021;12(1):1124.

[150] Yi X, Hu JJ, Dai J, Lou X, Zhao Z, Xia F, et al. Self-guiding polymeric prodrug micelles with two aggregation-induced emission photosensitizers for enhanced chemo-photodynamic therapy. ACS Nano 2021;15(2):3026–37.

[151] Zhu D, Zhang J, Luo G, Duo Y, Tang BZ. Bright bacterium for hypoxia-tolerant photodynamic therapy against orthotopic colon tumors by an interventional method. Adv Sci 2021;8(15):e2004769.

[152] Yu X, Zhang YC, Yang X, Huang Z, Zhang T, Yang L, et al. Bonsai-inspired AIE nanohybrid photosensitizer based on vermiculite nanosheets for ferroptosis-assisted oxygen self-sufficient photodynamic cancer therapy. Nano Today 2022;44:101477.

[153] Liu LH, Zhang XZ. Carrier-free nanomedicines for cancer treatment. Prog Mater Sci 2022;125:100919.

[154] Zhu L, You Y, Zhu M, Song Y, Zhang J, Hu J, et al. Ferritin-hijacking nanoparticles spatiotemporally directing endogenous ferroptosis for synergistic anticancer therapy. Adv Mater 2022;34(51):e2207174.

[155] Lei G, Zhuang L, Gan B. Targeting ferroptosis as a vulnerability in cancer. Nat Rev Cancer 2022;22(7):381–96.

[156] Zhu T, Shi L, Yu C, Dong Y, Qiu F, Shen L, et al. Ferroptosis promotes photodynamic therapy: supramolecular photosensitizer-inducer nanodrug for enhanced cancer treatment. Theranostics 2019;9(11):3293–307.

[157] Zhao LP, Chen SY, Zheng RR, Rao XN, Kong RJ, Huang CY, et al. Photodynamic therapy initiated ferrotherapy of self-delivery nanomedicine to amplify lipid peroxidation via GPX4 inactivation. ACS Appl Mater Interfaces 2022;14(48):53501–10.

[158] Huang J, Wang S, Zhou Y, Li Q, Yin J, Zha D, et al. Nanoformulations mediated metastasis brake in cancer therapy via photodynamic-enhanced ferroptosis and regional inflammation management. Chem Eng J 2023;451:138585.

[159] Yao X, Yang B, Wang S, Dai Z, Zhang D, Zheng X, et al. A novel multifunctional FePt/BP nanoplatform for synergistic photothermal/photodynamic/chemodynamic cancer therapies and photothermally-enhanced immunotherapy. J Mater Chem B 2020;8(35):8010–21.

[160] Jiang F, Ding B, Zhao Y, Liang S, Cheng Z, Xing B, et al. Biocompatible CuO-decorated carbon nanoplatforms for multiplexed imaging and enhanced antitumor efficacy via combined photothermal therapy/chemodynamic therapy/chemotherapy. Sci China Mater 2020;63(9):1818–30.

[161] Hao Y, Mao L, Zhang R, Liao X, Yuan M, Liao W. Multifunctional biodegradable prussian blue analogue for synergetic photothermal/photodynamic/chemodynamic therapy and intrinsic tumor metastasis inhibition. ACS Appl Bio Mater 2021;4(9):7081–93.

[162] van der Meel R, Sulheim E, Shi Y, Kiessling F, Mulder WJM, Lammers T. Smart cancer nanomedicine. Nat Nanotechnol 2019;14(11):1007–17.

[163] Pomeroy AE, Schmidt EV, Sorger PK, Palmer AC. Drug independence and the curability of cancer by combination chemotherapy. Trends Cancer 2022;8(11):915–29.

[164] Pan WL, Tan Y, Meng W, Huang NH, Zhao YB, Yu ZQ, et al. Microenvironment-driven sequential ferroptosis, photodynamic therapy, and chemotherapy for targeted breast cancer therapy by a cancer-cell-membrane-coated nanoscale metal-organic framework. Biomaterials 2022;283:121449.

[165] Zhang P, Liu C, Wu W, Mao Y, Qin Y, Hu J, et al. Triapine/Ce6-loaded and lactose-decorated nanomicelles provide an effective chemo-photodynamic therapy for hepatocellular carcinoma through a reactive oxygen species-boosting and ferroptosis-inducing mechanism. Chem Eng J 2021;425:131543.

[166] Zhang Y, Han X, Liu Y, Wang S, Han X, Cheng C. Research progress on nano-sensitizers for enhancing the effects of radiotherapy. Mater Adv 2022;3(9):3709–25.

[167] Liu J-Y, Liu N, Wu Y, Ning X-M, Zhang W-C, Qian J. NaErF4-based nanocarrier for enhanced ferroptosis therapy of cancer. ACS Appl Nano Mater 2023;6(1):270–82.

[168] Liu Y, Zhu X, Wei Z, Feng W, Li L, Ma L, et al. Customized photothermal therapy of subcutaneous orthotopic cancer by multichannel luminescent nanocomposites. Adv Mater 2021;33(30):e2008615.

[169] Zhao Y, Zhao T, Cao Y, Sun J, Zhou Q, Chen H, et al. Temperature-sensitive lipid-coated carbon nanotubes for synergistic photothermal therapy and gene therapy. ACS Nano 2021;15(4):6517–29.

[170] Cheng H, Wang X, Liu X, Wang X, Wen H, Cheng Y, et al. An effective NIR laser/tumor-microenvironment co-responsive cancer theranostic nanoplatform with multi-modal imaging and therapies. Nanoscale 2021;13(24):10816–28.

[171] Tao W, Wang N, Ruan J, Cheng X, Fan L, Zhang P, et al. Enhanced ROS-boosted phototherapy against pancreatic cancer via Nrf2-mediated stress-defense pathway suppression and ferroptosis induction. ACS Appl Mater Interfaces 2022;14(5):6404–16.

[172] Li X, Feng X, Sun C, Liu Y, Zhao Q, Wang S. Mesoporous carbonmanganese nanocomposite for multiple imaging guided oxygen-elevated synergetic therapy. J Control Release 2020;319:104–18.

[173] Chin YC, Yang LX, Hsu FT, Hsu CW, Chang TW, Chen HY, et al. Iron oxide@chlorophyll clustered nanoparticles eliminate bladder cancer by photodynamic immunotherapy-initiated ferroptosis and immunostimulation. J Nanobiotechnol 2022;20(1):373.

[174] Zhou Y, Fan S, Feng L, Huang X, Chen X. Manipulating intratumoral Fenton chemistry for enhanced chemodynamic and chemodynamic-synergized multimodal therapy. Adv Mater 2021;33(48):e2104223.

[175] Chen J, Chen F, Zhang L, Yang Z, Deng T, Zhao Y, et al. Self-assembling porphyrins as a single therapeutic agent for synergistic cancer therapy: a one stone three birds strategy. ACS Appl Mater Interfaces 2021;13(24):27856–67.

[176] Liao P, Wang W, Wang W, Kryczek I, Li X, Bian Y, et al. CD8(+) T cells and fatty acids orchestrate tumor ferroptosis and immunity via ACSL4. Cancer Cell 2022;40(4) 365–78 e6.

[177] Sun X, Cao Z, Mao K, Wu C, Chen H, Wang J, et al. Photodynamic therapy produces enhanced efficacy of antitumor immunotherapy by simultaneously inducing intratumoral release of sorafenib. Biomaterials 2020;240:119845.

[178] Broz P, Pelegrin P, Shao F. The gasdermins, a protein family executing cell death and inflammation. Nat Rev Immunol 2020;20(3):143–57.

[179] Ding Y, Ye B, Sun Z, Mao Z, Wang W. Reactive oxygen species-mediated pyroptosis with the help of nanotechnology: prospects for cancer therapy. Adv NanoBiomed Res 2022;3(1):2200077.

[180] Xu S, Zhou S, Xie L, Dou W, Zhang R, Zhao B, et al. A versatile NiS2/FeS2 hybrid nanocrystal for synergistic cancer therapy by inducing ferroptosis and pyroptosis. Chem Eng J 2023;460:141639.

[181] Guo R, Deng M, Li J, He X, He P, Liu H, et al. Depriving tumor cells of ways to metastasize: ferroptosis nanotherapy blocks both hematogenous metastasis and lymphatic metastasis. Nano Lett 2023;23(8):3401–11.

[182] Zhou S, Li D, Lee C, Xie J. Nanoparticle phototherapy in the era of cancer immunotherapy. Trends Chem 2020;2(12):1082–95.

[183] Hou B, Zhou L, Wang H, Saeed M, Wang D, Xu Z, et al. Engineering stimuli-activatable boolean logic prodrug nanoparticles for combination cancer immunotherapy. Adv Mater 2020;32(12):e1907210.

[184] Wang W, Green M, Choi JE, Gijon M, Kennedy PD, Johnson JK, et al. CD8(+) T cells regulate tumour ferroptosis during cancer immunotherapy. Nature 2019;569(7755):270–4.

[185] Wang Y, Sun T, Jiang C. Nanodrug delivery systems for ferroptosis-based cancer therapy. J Control Release 2022;344:289–301.